ELASTOMERIC SLEEVE BEARING DESIGN

ELASTOMERIC SLEEVE BEARING DESIGN

By

LAWRENCE FAFARMAN, B.S.M.E.

A Thesis

Submitted to the School of Graduate Studies

in Partial Fulfillment of the Requirements

for the Degree

Master of Engineering

McMaster University

March 1972

MASTER OF ENGINEERING (1972) McMASTER UNIVERSITY
(Mechanical Design) Hamilton, Ontario

TITLE: Elastomeric Sleeve Bearing Design

AUTHOR: Lawrence Milton Fafarman, B.S.M.E.
(University of California at Santa Barbara)

SUPERVISOR: Professor W. R. Newcombe

NUMBER OF PAGES: vi, 83

SCOPE AND CONTENTS:

It is shown that the experimentally determined deflectional behavior of certain elastomer-lined sleeve bearings under static radial loads can be modeled to some extent by the compressive behavior of flat elastomeric slabs.

An equation for the thermal bearing-bore change is developed using the conventional theory for the thermoelasticity of homogeneous cylinders. Some experimental results agree fairly well with this equation. An equation for the bore contraction due to liquid swell is developed in terms of thermoelasticity.

Minimizing the lining thickness is recommended for minimizing both the radial deflections and the bore changes.

An analysis is made of the frictional forces involved with the interference fit between the lining and its housing.

Areas for further investigation are suggested.

PREFACE

The main purpose of this thesis is to develop some basic design information for elastomeric sleeve bearings, which consist of elastomeric(i.e., rubberlike) linings in rigid housings. Although a particular elastomer trademarked "Thordon" is considered, the analysis here is intended to be applicable to other elastomers as well. In addition, the approaches used in the sections on clearances and interferences are also applicable to plastic-lined sleeve bearings. General knowledge of the elasticity of elastomers gives insight into the deflectional behavior of these sleeve bearings when under radial loads, so it is a secondary aim of this thesis to provide an elementary background in the elasticity of elastomers.

It is the author's opinion that the scarcity, or non-existence, of specific engineering knowledge on elastomeric sleeve bearings greatly increases the chances of their being misapplied or poorly designed, and discourages their selection as a superior choice for many abrasive operating environments. It is hoped, therefore, that this thesis will fill a definite engineering need.

The thesis is divided into the following three main subjects:

(1) Load deflections of elastomeric sleeve bearings;

(2) Clearances;

(3) Interference fit with housing.

ACKNOWLEDGMENTS

The author would like to thank the following men for their invaluable assistance in this project: his supervisor, Prof. W. R. Newcombe, for patient counseling throughout the course of the project; Dr. M. Levinson, also of McMaster University, for his many helpful hints and clarifications; Mr. G. Thomson, of Thomson-Gordon Ltd. of Hamilton, for providing test material and practical advice.

This work was financially supported by the National Research Council of Canada.

TABLE OF CONTENTS

PAGE

1. LOAD DEFLECTIONS OF ELASTOMERIC SLEEVE BEARINGS

1.1 INTRODUCTION

An elastomeric sleeve bearing(Fig. 1.1) will deflect significantly under heavy radial loads, even if a stiff elastomer is used. For example, a Thordon bearing of originally recommended wall thickness(about one-tenth the shaft diameter) and under a radial projected-area pressure of 2,500 psi generally deflects in the neighborhood of 4% of wall thickness. Though deflection is, of course, necessary in the bush-type rubber mountings used as springs and vibration isolators, it is usually undesirable in rotational bearings, where deflections can produce harmful static and vibrational stresses in shafts or in the elastomeric lining itself and affect the alignment of attached gears and other precision parts, though exceptions are the cases where the bearing is deliberately employed to accommodate misalignment or to absorb shocks. It is obvious, therefore, that a designer might require knowledge of the load-deflection behavior of elastomeric sleeve bearings and also, if possible, of means of controlling the deflection to some extent. Unfortunately, however, current engineering literature is deficient in such knowledge, and it is one of the main purposes of this thesis to help correct this.

It should be pointed out now that the predictions of radial bearing deflection to be given here should only be

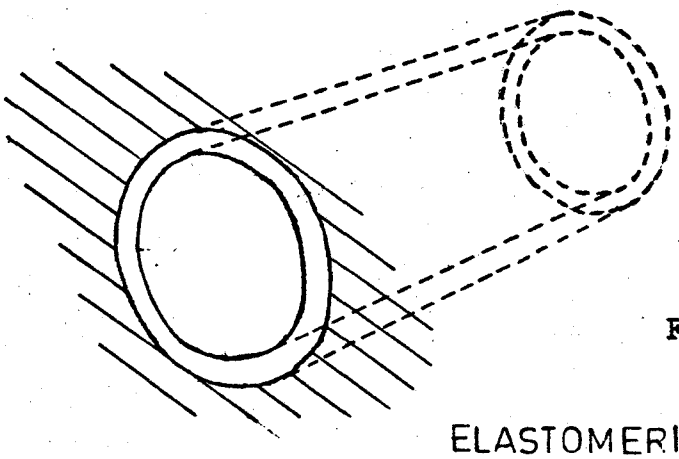

FIG. 1.1

ELASTOMERIC SLEEVE BEARING

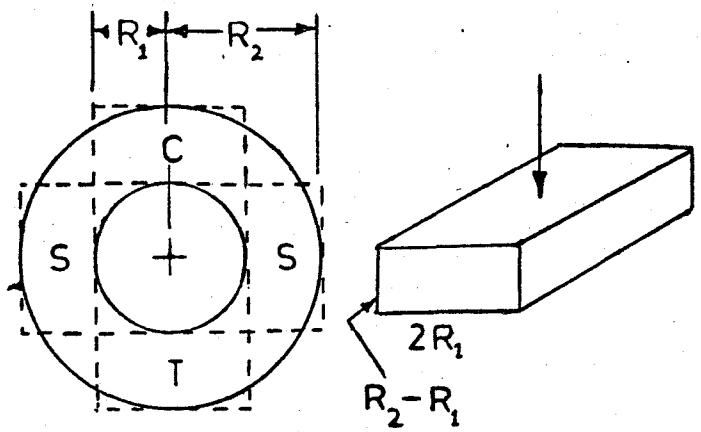

FIG. 1.2

APPROXIMATE SOLUTION FOR RADIAL STIFFNESS OF BONDED RUBBER BUSHINGS

FROM FIG. 4-17, PAGE 83 OF REF. 1

expected to be rough guides because of the following reasons:

(1) The effect of the surface contact conditions, at both the bearing surfaces and at the interface between the lining and the housing, upon the lining's deflection. This effect is difficult to control in laboratory tests as well as in practical applications.

(2) The high creep of Thordon makes the loading history an important factor, and the loading history is difficult to accurately control in tests and might be impossible to control in the field.

(3) From a practical standpoint, extreme accuracy in predicting deflection due to load would not be justified, anyway, in those situations where this deflection would be negligible compared to the other factors affecting alignment, namely wear and the large bearing clearances which are required to offset thermal and liquid-swell expansions and to provide smooth running. These other factors alone would generally be sufficient to prohibit use where extremely accurate shaft alignments are required.

1.2 ANALOGIES FOR ELASTOMERIC DEFLECTIONS

One possible way of providing deflection data is to run deflection tests on every conceivable combination of bearing specifications, varying the length, diameter, wall thickness, perhaps the bearing clearance, and also the surface contact conditions where the elastomer contacts the shaft and the surrounding housing- the amount of interfacial slippage allowed by the surface conditions can have a large effect on the radial stiffness of the bearing. However, a more efficient, and illuminating, method would be to attempt to analogize the compressive behavior of the sleeve bearing lining to that of some simple shape for which there is already extensive theoretical and experimental knowledge on compression or for which such knowledge can be readily determined. This idea of analogy is not new; it was summed up by McPherson and Klemin[1] as follows:

> For shapes in which the load bearing faces are not equal and parallel as required for the direct application of the shape factor the stiffness may be calculated by calculating the stiffness of one or more shapes approximating as closely as possible the desired shape. For example, a tapered piece or a truncated cone may be considered as having a load face equivalent to the average of the actual load faces. A dome-shaped bumper may be considered as a truncated cone. Such approximations as these may be very rough, but they serve to establish a size for experimental checking.

McPherson and Klemin[2] then proceed to give the following example:

> A special case that is frequently encountered relates to the radial deflection of a bushing adhered between cylindrical surfaces having a common axis at no load. The hollow cylinder of rubber may be considered as represented by four equal blocks of rubber as shown

in Fig.(1.2), one being in compression, one in tension, and two in shear. The combined stiffness may be calculated by combining spring rates, or constants, as they are more correctly termed, but a good approximation is 1.5 times the stiffness of a block in compression having a thickness R_2-R_1 , a width $2R_1$, and a length equal to that of the bushing.

Unfortunately, the above analogy, though it appears to be closely related to the problem at hand, was not considered immediately applicable because of different surface conditions; the bush-type mountings considered above are effectively bonded at both interfaces whereas the bearing can at most be bonded at only one, introducing the surface condition effect mentioned previously. Another difference is that in the case of the bearing, there would be little contribution from shear and none from tension because of the lack of a bond. However, the same basic concept is employed for the analogy to be developed here.

Another, similar analogy for a bonded bush-type mounting is given by Harris and Crede[3]. This analogy differs from the first mainly in neglecting the shear and tension contributions, which, according to the first, increase the stiffness by one-half.

In fact, in the absence of actual results for sleeve bearings, the Thordon sales brochure used a rough analogy similar to those given above, but without regard to shape factors or surface conditions; the estimate of a deflection of 4% of wall thickness at 2,500 psi projected-area pressure, based on available data for a bonded flat disc, was, as it

turned out, with some coincidence, fairly good.

The last helpful example of an analogy is the experimental proof that a rubber ring under axial or radial loads(see Fig. 1.3) behaves similarly to an equivalent compressed straight cylinder, bonded at the ends, that would be formed by cutting the ring and unrolling it.[4]

The purpose of the next section is to develop the background in rubber elasticity necessary for understanding the sleeve bearing analogy to be used in this thesis.

RUBBER RING COMPRESSED RADIALLY AROUND CIRCUMFERENCE

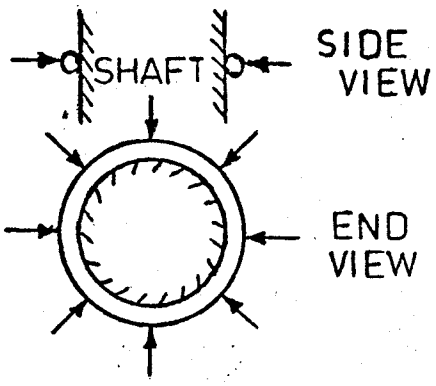

AXIAL COMPRESSION OF RUBBER RING

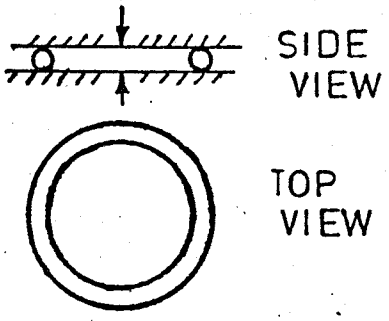

FIG. 1.3

RADIAL LOADING OF RUBBER CYLINDER, WITH CONSTRAINT AGAINST BULGING AT ENDS

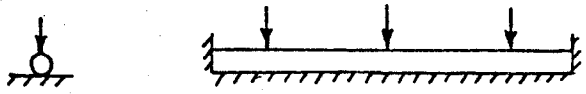

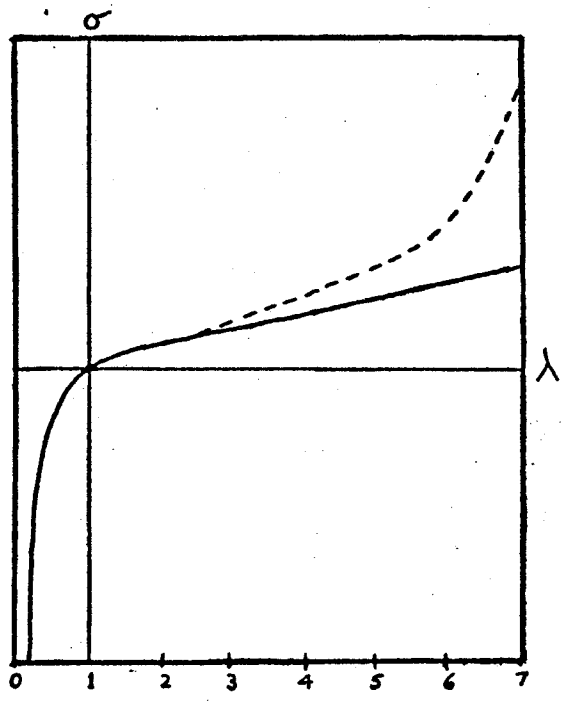

FIG. 1.4

FORCE VS. RELATIVE LENGTH FOR RUBBER STRESSED IN TENSION AND COMPRESSION

—— THEORETICAL, $\sigma = G(\lambda - \lambda^{-2})$

- - - OBSERVED

1.3 ELASTICITY OF ELASTOMERS

1.3.1 Introduction

The elasticity of elastomers is a very broad and involved subject, including such important areas as large strain theory and dynamic behavior. However, this thesis will concentrate on what is here the most relevant area- compressive elasticity. No prior knowledge of elastomeric elasticity on the part of the reader is assumed. Although the more familiar term rubber is usually used below, it refers to elastomers in general.

1.3.2 General Elastic Properties

No introduction to rubber elasticity would be complete without at least passing mention of rubber's special, often unique, elastic properties. The most obvious, but by no means trivial, property is the ability to stretch to a great extent, often several hundred percent, and to recover more or less completely on release. Some of the other most useful properties, such as high abrasion resistance and energy storing ability, are derived from that property. The following are some of the lesser-known properties:

(1) Energy storing ability- rubber can store 150 times as much energy as an equal weight of tempered steel[5]

(2) Creep- this may be noted whenever rubber is subjected to stress if sufficiently precise observations are made, in contrast to metals, where creep seems to occur only under

relatively high stress or at elevated temperatures.

(3) Non-linearity of elasticity- Hooke's law of the proportionality between stress and strain does not hold for rubber in general; it does, however, hold approximately for relatively low elongations, e.g., of the order of a few percent.

(4) Set- related to creep- set in rubber may or may not recover more or less completely with time, whereas set in metals is irreversible.

(5) Incompressibility- it may come as a surprise to many people, but despite solid rubber's great general flexibility, when constrained against bulging it is practically rigid in compression; that is, rubber has a high ratio of bulk modulus to Young's modulus, giving rubber a Poisson's ratio of very nearly one-half.

(6) The Gough-Joule effect[6]- the name given to the possible increase in rubber's stiffness with an increase in temperature, in contrast to the opposite effect with metals; however, when temperature is low or deformation rate high, so that equilibrium is not attained, the Gough-Joule effect is no longer the governing factor determining temperature dependence- at very low temperatures, rubbers in general freeze to a glassy solid; when temperature is high, increased creep rates tend to lower the apparent stiffness of the rubber.

1.3.3 Stress-Strain Relations

Considerable confusion might be caused by the fact that the stress-strain relationship for rubber is expressed in two different ways, one way being the familiar linear Hooke's law, suitable for the relatively small deformations which are of greater interest here, the other accommodating the non-linear behavior of large strains. However, since the latter formulation is quite common in the rubber literature and since it gives the more general picture of rubber elasticity, it, too, will be discussed here, and its agreement with Hooke's law at small deformations will subsequently be shown.

Hooke's law may be assumed to hold for compressive strains in rubber up to about 10-20%, i.e.,[7]

(1.1) $\sigma = Ee$

-where

σ = stress. Because of small deformation, no distinction is necessary here between initial and final cross-sections when calculating stress; compare with the definition in the nonlinear formulation.

E = Young's modulus. Because of the non-linearity of rubber's stress-strain curve at large deformations, the term modulus as applied to rubber often has a different meaning. For example, if a tensile stress of 1,800 psi produces an elongation of 300%, the rubber is said to have a 300% modulus of 1,800 psi. However, let E here be the compression modulus for homogeneous compressions. A homogeneous compression, shown in Fig.(1.5A), is one where the contact faces are perfectly lubricated and thus completely free to slip, so that a flat slab in compression will not bulge at the sides; it is called homogeneous because

all body elements are in the same state of stress and strain. Furthermore, let E be taken as the slope of the stress-strain curve at the origin.

e = elastic strain.

The nonlinear form[8] is given below:

$$\sigma = G(\lambda - \lambda^{-2}) \tag{1.2}$$

-where

σ = stress calculated on the basis of the original undeformed cross-section(the engineer must be careful to note that the rubber technologist's stress-strain curve always has the stress calculated in this way).

G = shear modulus(also called the modulus of rigidity)

λ = relative length- the ratio of strained to unstrained length, the length being the dimension in the direction of deformation(note that this is not the same as the engineering elastic strain e, which is the ratio of the difference of the strained and unstrained lengths to the unstrained length; that is, $\lambda = 1+e$).

A graph of Eq.(1.2) is shown in Fig.(1.4). It should be noted that the drawing of the compression part of this curve as a smooth continuation, through the origin, of the tension part assumes that the compression is homogeneous(Fig. 1.5A).

Experiments confirm that Eq.(1.2) and Fig.(1.4) are reasonable representations of the behavior of rubber except at fairly high elongations, where the deviation is indicated by the dotted line in Fig.(1.4). However, this deviation is not of concern here.

G and E are related by the following equation:[9]

$$G = \frac{E}{2(1+\nu)}$$

-where ν, Poisson's ratio, is about $\frac{1}{2}$ for rubber. Therefore, the value $\nu=\frac{1}{2}$ will be used, making

$$(1.3) \quad G = \frac{1}{3}E$$

Substituting Eq.(1.3) and the relation $\lambda=1+e$ into Eq.(1.2) gives

$$(1.4) \quad \sigma = \frac{1}{3}E(1+e-(1+e)^{-2})$$

Expanding $(1+e)^{-2}$ in a binomial series(assuming $e<1$, which is certainly true for small strains),

$$(1.5) \quad \sigma = \frac{1}{3}E(1+e-(1-2e+3e^2-4e^3+---))$$

For small strains, terms of e^n, $n>1$, may be neglected. Eq.(1.5) then reduces to

$$\sigma = Ee$$

-which is simply Hooke's law, Eq.(1.1).

1.3.4 Compressive Elasticity

1.3.4.1 Shape Functions and Shape Factors

It should first be reemphasized that the compressive behavior of rubber depends to a great degree on the amount of slippage between the rubber and the compression faces and on any other constraint limiting free sidewise expansion or bulging of the rubber. Some different situations are shown in Fig.(1.5), in order of increasing stiffness, (A) to (D). Fig.(1.6) shows quantitatively the effect of different contact-

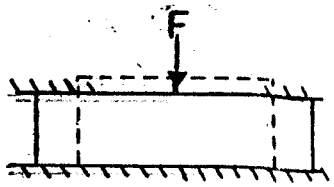

(A) FREE SLIPPAGE ALONG COMPRESSION FACES (HOMOGENEOUS COMPRESSION)

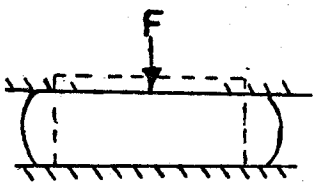

(B) PARTIAL SLIPPAGE ALONG COMPRESSION FACES

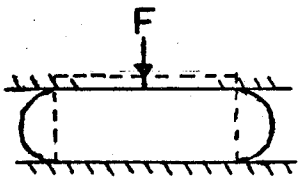

(C) NO SLIPPAGE ALONG COMPRESSION FACES, DUE TO BOND OR HIGH FRICTION

FIG. 1.5

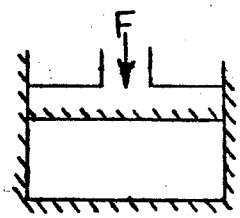

(D) COMPLETE CONSTRAINT; "POT BEARING"

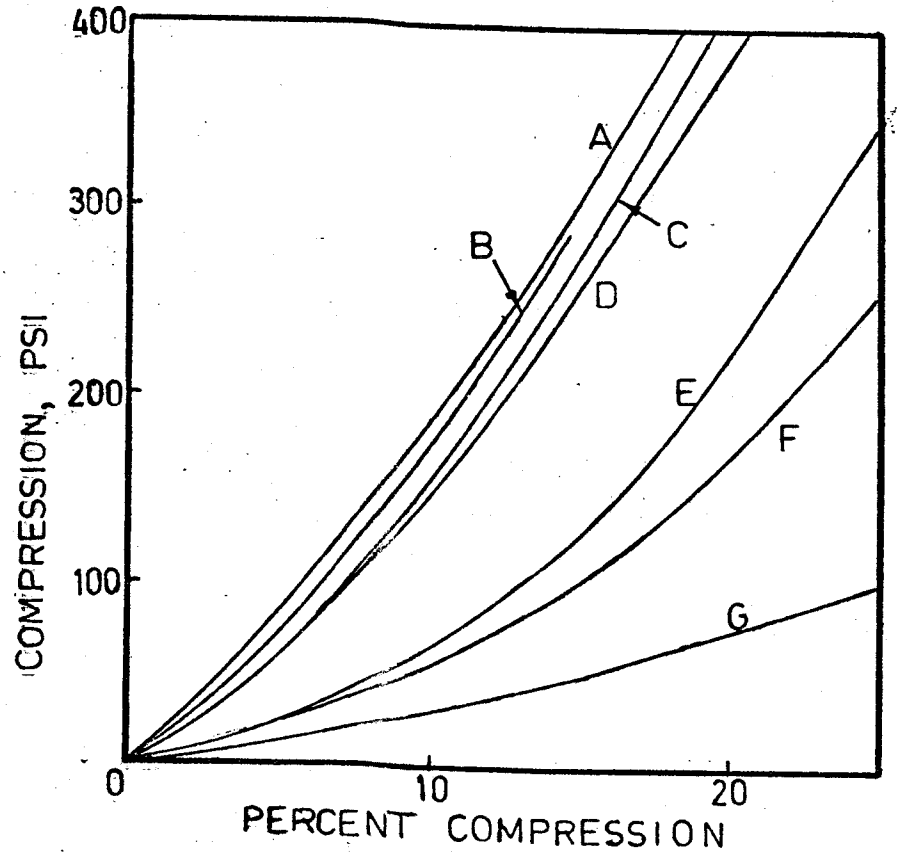

SURFACE CONDITION

A - BONDED
B - SANDPAPER
C - DRY AND CLEAN
D - SULPHUR
E - POWDERED TALC
F - GRAPHITE
G - PETROLATUM

FIG. 1.6

EFFECT OF SURFACE CONDITION ON THE COMPRESSIVE STIFFNESS OF A RUBBER SLAB. FROM PAGE 81 OF REFERENCE 1.

face conditions on the stress/deflection curve for a typical rubber specimen under compression. Condition A (bonded) in Fig.(1.6) corresponds to Fig.(1.5C). Note that because of the excellent gripping ability of typical rubbers, even the friction against dry, clean, polished steel can behave here almost as a bond.

It is apparent from Fig.(1.6) that any unpredictability (for example, that caused by uncertainty about the amount of lubrication present) as to the amount of slippage at the contact surface would make it impossible to accurately predict the deflection curve. Fortunately, however, Fig.(1.6) indicates that for deflections of the order of magnitude generally concerning these bearings(under 5%), the effect of slippage is relatively much less severe than for large deflections; this was confirmed in tests on Thordon. At any rate, the surface condition that has received most of the experimental and theoretical work for compression is the bonded one because this type gives the most reproducible results and because many important applications, such as rubber shock mountings and vibration isolators, use bonds.

As discussed in the last section, Hooke's law may be assumed to hold for homogeneous compressions up to about 10-20% strain:

$$\sigma = Ee \tag{1.6}$$

The difference in compressional stiffness between a

slab in homogeneous compression(Fig. 1.5A) and the same slab with bonded faces(Fig. 1.5C) may be accounted for by the so-called shape function S in the following equation:

$$\sigma = ES \cdot e \qquad (1.7)$$

or

$$\sigma = E_a e \qquad (1.7a)$$

In a comparison between Eqs.(1.6), (1.7), and (1.7a), S may be considered to modify the original Young's modulus E to form an "apparent" compression modulus E_a, which represents the compressive stiffness of bonded slabs. Some formulas for S are given in Table(1.1). It is apparent that the shape function depends on the slab's relative thickness, on the modulus or hardness of the rubber, and on the cross-sectional configuration, in decreasing order of importance(The effect of bulk compressibility for very thin or stiff slabs, to be discussed in Sec. 1.3.4.2, is not, however, accounted for by these shape functions. There the compressive stiffness of the slab is actually lower than Eq. 1.7 and Table 1.1 indicate). The effect of relative thickness, being the most important, is described by another expression, the so-called shape factor s, defined as follows:

$$s = \frac{\text{Loaded Area}}{\text{Free Area}} \qquad (1.8)$$

The Free Area is the unloaded area at the sides which is free to bulge as in Fig.(1.5C); the Loaded Area is that

Expressions For Shape Function

In all formulae h = height, i.e. in direction of compression

Cross-section	Shape function	Variation of B, C, and D with shear modulus G, lb/in²				
Square side = a	$1 + B(a/h)^2$					
		$G < 100$	100–150	150–200	200–300	> 300
Circular diameter = d	$1 + B(d/h)^2$	B 0·120	0·103	0·080	0·063	0·056
Rectangular long side = l short side = w	$\frac{1{\cdot}33 + 0{\cdot}66w/l + C(w/h)^2}{1 + w/l}$	C 0·26	0·225	0·175	0·14	0·12
		D 0·065	0·056	0·044	0·035	0·030
Annulus outer diameter = d_2 inner diameter = d_1 *Case* 1: d_2 much greater than d_1	$1 + B(d_2 - d_1)^2/h^2$					
Case 2: d_1 almost as large as d_2	$1{\cdot}33 + D(d_2 - d_1)^2/h^2$					
Hollow Square outer side = a_2 inner side = a_1 Case 1: a_2 much greater than a_1	$1 + B(a_2 - a_1)^2/h^2$					
Case 2: a_1 almost as large as a_2	$1{\cdot}33 + D(a_2 - a_1)^2/h^2$					

(Note: these symbols differ from those used in this thesis)

TABLE 1.1

Taken from Davey & Payne[10]

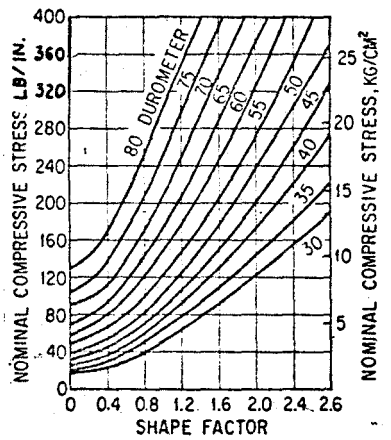

From Harris & Crede[11]

FIG. 1.7

Loads for 10 per cent deflection for rubber specimens having various hardness values and shape factors.

of the cross-section perpendicular to the direction of compression. The relationship between the shape factor and the compressive stiffness of rubber slabs is shown in Fig.(1.7).[11] Shape factor graphs such as Fig(1.7) are often determined experimentally; on the other hand, Gent and Lindley[12] derive some shape functions theoretically.

The distinction between the shape function and the shape factor should be kept clear. The shape function is intended to be a coefficient representing the ratio between the compressive stiffness of a slab with both faces bonded and that of the same slab in homogeneous compression, whereas the shape factor is a function only of the geometry of the slab. If desired, the shape factor might be incorporated into the shape function by making the appropriate dimensional substitutions in Table(1.1)(alternatively, the shape functions can be regarded as mathematical expressions of shape factor graphs). However, the shape factor is often used in graphs such as Fig.(1.7), which are useful where the elastomer does not obey a simple shape function. Also, the shape functions as given in Table(1.1) automatically take into account the cross-sectional configuration's effect, which is often neglected in presentations of the shape factor; this effect is discussed next, as the similarity rule.

Hooke's law(Eq. 1.1) says, of course, that in homogeneous compression any two flat slabs of equal Young's modulus will have the same percentage deflection(i.e.,

strain) under equal compressive loads per unit area(i.e., stress), regardless of their shapes. According to the similarity rule, the same is true of two bonded slabs which are geometrically similar, that is, of the same shape but different size. When the similarity rule fails to hold in actual tests, the cause will be found in some difference in the rubbers or in the experimental conditions[13] The similarity rule may also be applied to two bonded slabs of different shape but equal shape factor, with the limitation that narrow thin strips are somewhat softer than their shape factors would indicate- strips with a length-width ratio of 10:1 were determined to be about 22% softer[14] than discs of corresponding shape factor. This exception to the similarity rule will be relevant to the analogy to be developed here for elastomeric sleeve bearings.

1.3.4.2 Bulk Compressibility

Noting how the shape functions in Table(1.1) increase without limit as the slab becomes relatively thinner(i.e., as the shape factor becomes higher), it would thus seem that, in theory, a slab could be given an infinitley high apparent compression modulus by making it infinitesimally thin. In actuality, however, bulk compressibility exerts a law of diminishing returns here, limiting the apparent stiffness as explained below.

Gent and Lindley[15] have pointed out and demonstrated

by actual measurements that where the bulk compression becomes significant the total compressive strain e_t must be calculated as the sum of the elastic strain e (as given by Eq. 1.7) and the volume strain e_b:

(1.9) $$e_t = e + e_b$$

The bulk modulus K is defined as follows:

(1.10) $$K = \frac{(1/3)(\sigma_x+\sigma_y+\sigma_z)}{e_x+e_y+e_z}$$

-where the numerator of Eq.(1.10) is σ_m , the mean normal stress, and, assuming small strains, the sum of strains given in the denominator is the volume compression, $\Delta V/V$.

If the "pot bearing" of Fig.(1.5D) were filled with fluid and the x-axis were taken as the direction of compression, then, using the property that a fluid transmits pressure equally in all directions,

$$\sigma_x = \sigma_y = \sigma_z = \sigma_m = -p$$

-where p is the hydrostatic pressure

It would also be true that

$$e_b = e_x \quad \text{and} \quad e_y = e_z = 0$$

Eq.(1.10) could then be written

(1.11) $$e_b = \Delta V/V = \frac{-p}{K}$$

Now, the rubber-filled pot-bearing may not be a case of true hydrostatic compression; however, if the assumption is made that σ_m is here proportional to the external applied

stress σ, then

(1.12) $$e_b = \frac{\sigma}{K_e}$$

-where K_e is an "effective" bulk modulus.

Consider next the case of a bonded slab, Fig.(1.5C). As the slab becomes thinner, bulging is reduced relative to the slab's volume and the slab thus approaches the pot bearing condition. For this reason, it is assumed that Eq.(1.12) is also a good approximation for thin bonded slabs.

Defining a new "apparent" compression modulus, E_a', in terms of the total strain e_t, that is,

(1.13) $$\sigma = E_a' e_t$$

Eq.(1.9) then becomes, using Eqs.(1.7a),.(1.12), & (1.13),

(1.14) $$\frac{1}{E_a'} = \frac{1}{E_a} + \frac{1}{K_e}$$

Defining a new quantity n as the ratio between E and K_e (if K_e were K, this ratio would be $1/(3(1-2\nu))$, according to the relations between the elastic moduli[16]),

(1.15) $$K_e = n \cdot E$$

Using Eqs.(1.7) and (1.15), Eq.(1.14) can be written

(1.16) $$E_a' = E \left(\frac{1}{S} + \frac{1}{n}\right)^{-1}$$

-where S is the shape function, not the shape factor. Leaving Eq.(1.16) in terms of the shape function is the most general form, as the equation would vary for different rubber properties and different cross-sectional configurations if

written in terms of shape factors.

Defining an "apparent" shape function, S_a, associated with the new apparent compression modulus modulus E_a', in a manner analogous to the definition of the shape function S,

(1.17) $$E_a' = S_a E$$

-where S_a, unlike S, takes into account bulk compressibility.

A comparison of Eqs.(1.16) and (1.17), gives

(1.18) $$S_a = \frac{1}{\frac{1}{S} + \frac{1}{n}} \quad \text{or} \quad \frac{1}{S_a} = \frac{1}{S} + \frac{1}{n}$$

As the slab becomes thinner, $1/S \to 0$. From Eqs.(1.18), (1.17), & (1.15), it is seen that as $1/S \to 0$, $S_a \to n$ and $E_a' \to K_e$. Thus, after a certain point, further thinning of the slab should result in essentially no increase in the apparent compression modulus E_a' (however, it should be noted that this refers to relative or percentage stiffness, not to absolute deflections. The latter should continue to decrease as the slab is made thinner).

1.4 AN ANALOGY FOR SLEEVE BEARING DEFLECTIONS

The purpose of this analogy is to determine the bearing's approximate equivalents to the shape factor and compressive stress of flat slabs so that the deflectional behaviors of bearings and slabs can be compared. Three examples of analogies for rubber deflections were given in Sec.(1.2). Of these, the analogy to be presented here bears the most resemblance to the one of Harris & Crede,[17] the major changes being the consideration of unbonded surface conditions and correlation to a slab of practically infinite length rather than to one of the dimensions indicated in Fig.(1.2).

It seems reasonable to assume that the compressed area of the lining is effectively constrained, by the unloaded side of the lining, against "bulging" in the circumferential direction; this compressed area thus seems approximately equivalent to a flat rectangular area(see Fig. 1.8) free to bulge at the sides but constrained at the ends as in the last analogy[18] given in Sec.(1.2). Unfortunately, however, the compressive behavior of that particular slab was not found in the literature, so special tests, similar to those performed in the case of reference 19, would have been desirable. However, the analogy to the sleeve bearing was finally regarded as a segment of a practically infinitely long strip(Fig. 1.8), where the remoteness of end effects, causing vertical transverse planes to remain vertical, is more or less equivalent to the end constraints; this slab has the advantage of being

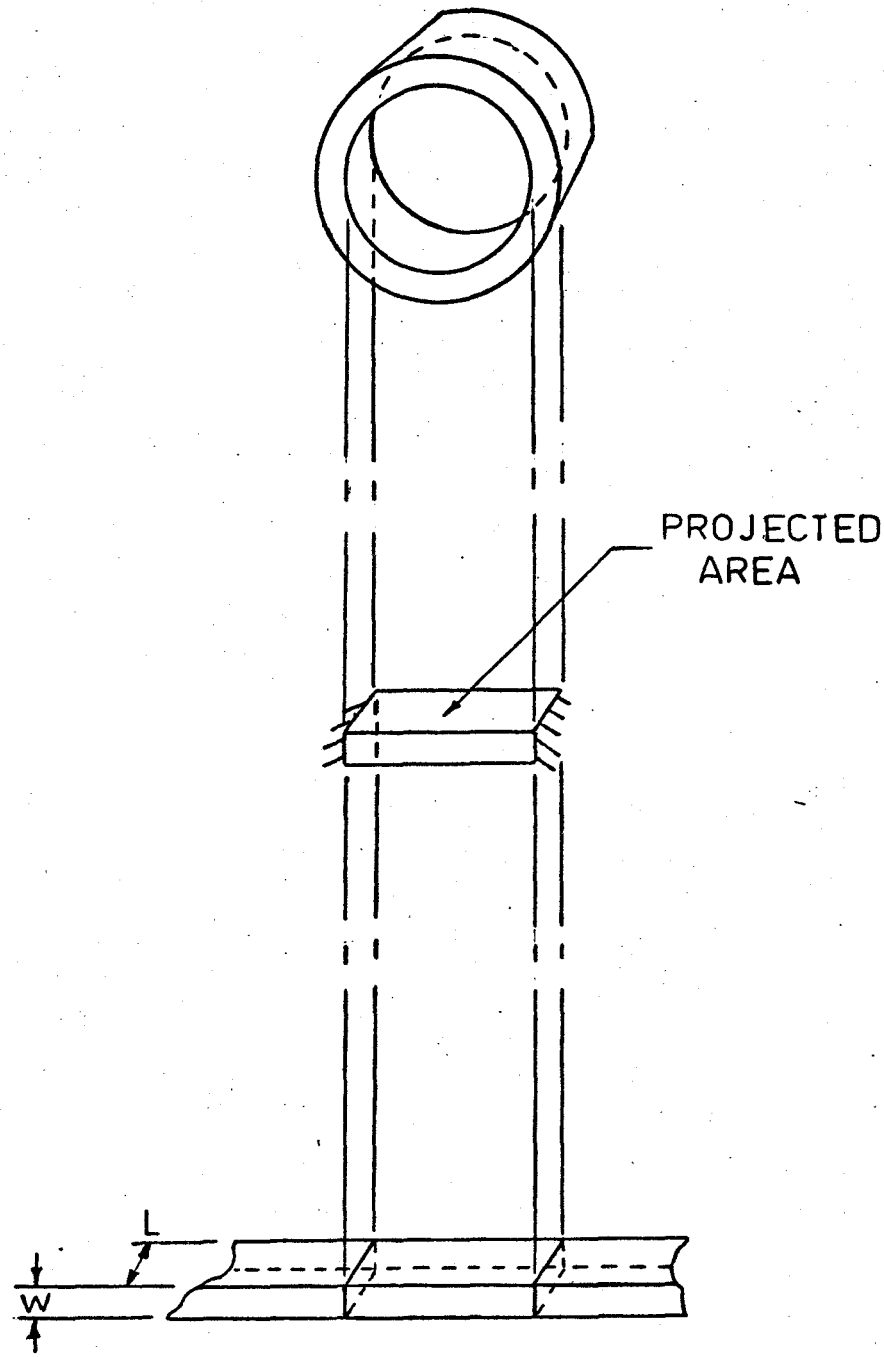

FIG. 1.8

discussed in the literature. The next question was whether to attempt to use a shape function for the strip or to use the shape factor concept. The shape factor was selected for the reasons stated below.

Shape functions for infinitely long rectangular slabs are given by Gent & Lindley[20] or can be derived from the shape function for rectangular slabs, Table(1.1), by taking the limit as the length goes to infinity. However, the shape function approach was rejected for the following reasons:

(1) These shape functions are intended for slabs bonded on both faces, a situation for which the sleeve bearing has no counterpart because the bearing surface must be free to slip.

(2) At any rate, the experimental compressive behavior of Thordon discs of shape factors equivalent to those of typical bearing linings deviated considerably from Eq.(1.16), and an attempt to develop and verify new theory would have been an undertaking beyond the scope of this thesis.

It is true that the shape factor and the similarity rule(Sec. 1.3.4.1) were also originally discussed here with regard to double-bonded slabs. However, that restriction is overcome here by assuming that a similarity rule also applies to other combinations of surface conditions; that is, two articles of different shape but equivalent in shape factor would be expected to have approximately the same apparent compression modulus so long as they had the same surface

conditions. The shape factor is thus to be used here mainly as a basis for comparison between different shapes rather than as an indicator of the effect of relative thickness on the stiffness of bonded slabs.

If L and w denote the width and height, respectively, of the strip at the bottom of Fig.(1.8), with L corresponding to the length of the bearing and w to the lining thickness, and also if l represents an arbitrary length along the strip, then the equivalent shape factor of the bearing becomes

$$(1.19) \qquad s = \frac{\text{Loaded Area}}{\text{Free Area}} = \frac{Ll}{2lw} = \frac{L}{2w}$$

In the actual deflection tests, discs were substituted for the long strip. However, according to the similarity rule at the end of Sec.(1.3.4.1), the discs should be almost equivalent to the long strip as regards the effect of shape factor; hence, Eq.(1.19) will be used to directly correlate sleeve bearings with discs.

The symbol σ_p shall be used to denote the "projected-area" pressure or stress, defined as the quotient of the division of the total radial force by the projected area (the top area of the slab in the middle of Fig.1.8); it is a rough estimate of the typical bearing pressure. Incidentally, the projected-area pressure multiplied by the surface velocity forms the "P-V" limit, which is a measure of a bearing's ability to dissipate and withstand the frictional

heat generated. In this thesis, however, σ_p is to be used along with the shape factor to correlate sleeve bearings with discs; σ_p for the sleeve bearings is to be considered roughly equivalent to the calculated compressive stresses for the discs, permitting a direct comparison of the deflection curves for the bearings with those for the discs. Sec.(1.5), which follows, describes how these deflection curves were determined.

1.5 MEASUREMENTS OF DEFLECTIONS

1.5.1 Discs

A few representative flat discs were tested in compression for the following reasons:

(1) Discs involve fewer experimental and theoretical variables than do elastomeric sleeve bearings.

(2) Many of their experimental variables are easier to control than are those of the sleeve bearings.

(3) They provide a more direct comparison with present knowledge on compressive behavior than do the sleeve bearings.

(4) They are easier to prepare for testing than are the sleeve bearings, requiring no housing, no slow, painstaking lathe turning or boring, and no special test jig.

(5) They provide insight into the deflectional behavior of the sleeve bearings in accordance with the analogy of Sec.(1.4).

Thordon Regular(Thordon is made in three grades-Regular, XL, and Super XL, the latter two containing a special anti-friction additive) discs of three different shape factors were compression tested by placing them between the loading faces of a compression-testing machine(Tinius-Olsen by make); the two higher shape factors are roughly in the same range as the equivalent shape factors of typical bearings. The discs were cut from stock-diameter rods and the thinnest size was machined flat by an end mill in a vertical milling machine,

a uniform thickness being assured by keeping each area pressed flat against the table while being cut; the thicker discs were held in a lathe chuck, with a section of rod behind for support, while being cut to final size. The test results, for different surface conditions, are graphed in Figs.(1.9), (1.10), & (1.11); σ, the average compressive stress, is based on the initial cross-sections, as is customary. The testing machine had a built-in load-measuring device; the deflections were measured with a dial gauge placed under the compression crosshead of the machine and as close as possible to the disc to minimize the error introduced by the deflections of the testing machine itself- nonetheless, the test results were corrected for the machine deflections, which were determined by applying the loads without a testpiece being present(Alternatively, small hole gauges might be used to directly measure the gap corresponding to the slab's thickness). For each test, σ was raised steadily in the following sequence, with the deflection being measured at each level: 500, 1000, 1500, 2000, 3000, 4000, 5000, & 6000 psi. A pause of about 10 seconds was made at each level, just long enough for a reading to be taken; the timing has an important bearing on the results because of the rapid stress-relaxation (associated with creep) that was observed. Each curve was drawn by visually smoothing data points that were averages of two test runs. A few general, qualitative observations

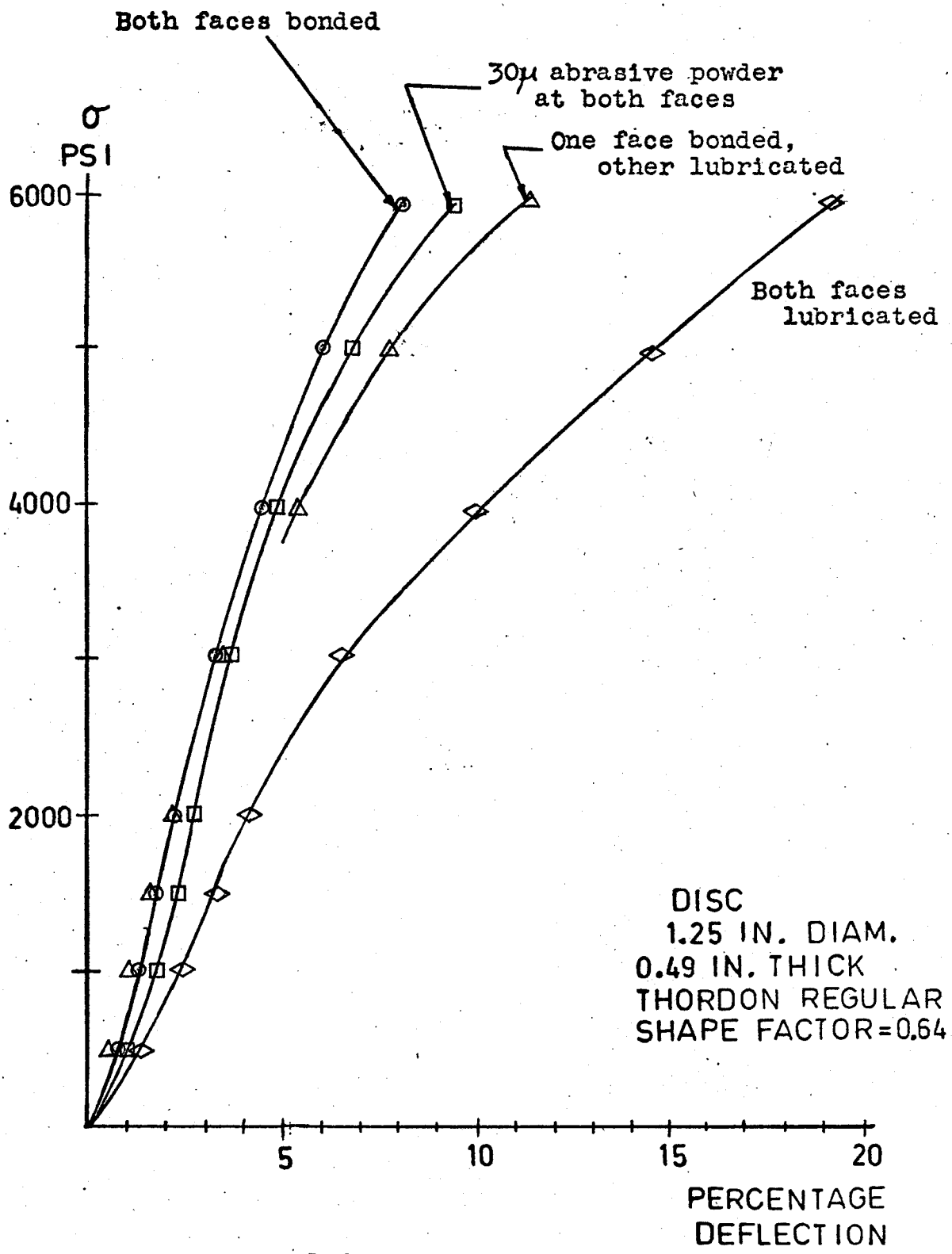

FIG. 1.9

COMPRESSION TESTS

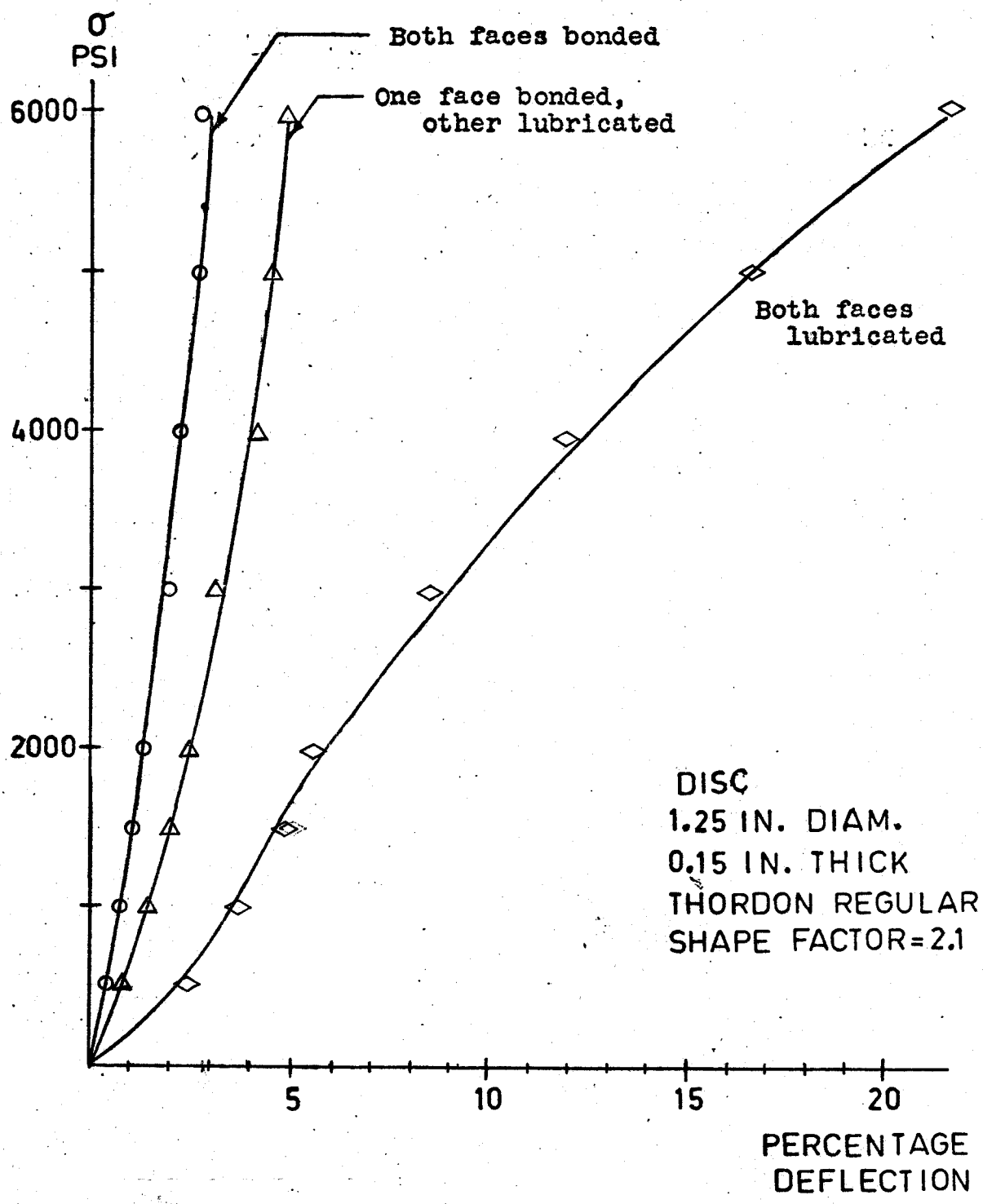

FIG. 1.10

COMPRESSION TESTS

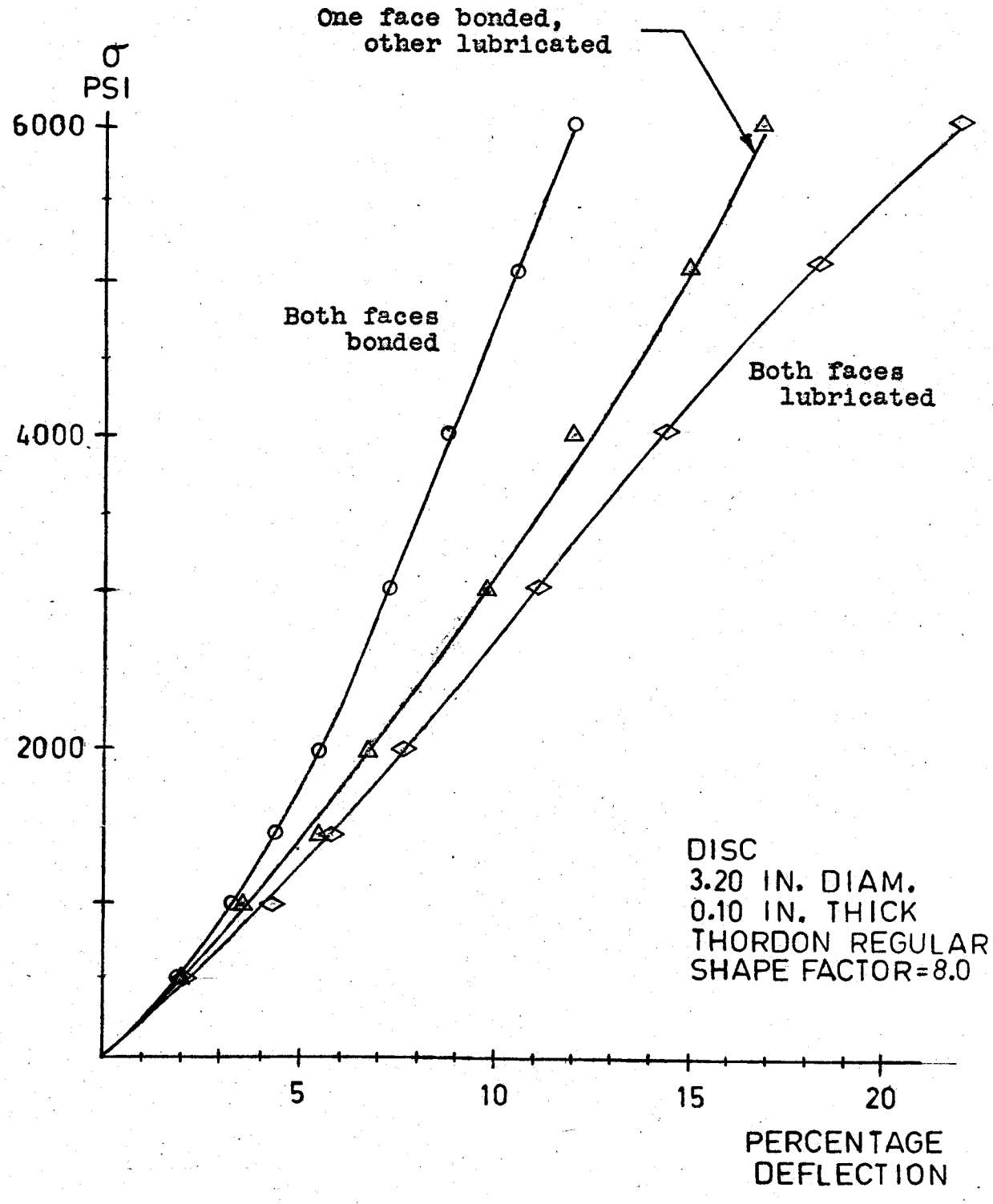

FIG. 1.11

COMPRESSION TESTS

about the results will be made below.

First, note that, in keeping with Eq.(1.6), the curves for the homogeneous compressions(both faces lubricated) in Figs.(1.9), (1.10), & (1.11) are almost identical despite the great differences in shape factor. The homogeneous compression curves for the two thicker discs show a softening at the largest measured deflections, whereas the compressive side of Fig.(1.4) indicates a stiffening with increasing deflection; this discrepancy is possibly due to the high creep property of Thordon. Each disc experimentally showed a fairly high apparent shape function S_a(the true ratio between the compressive stiffness of a slab bonded on both faces and that of the same slab in homogeneous compression), in general agreement with Fig.(1.6). S_a for the disc of Fig.(1.10) is considerably higher than that for the disc of Fig.(1.9), as would be predicted by Eq.(1.7) and Table(1.1) if the reasonable assumption were made that the latter disc is too thick for bulk compressibility to be predominant.

An unexpected result is that the thinnest disc has the lowest measured S_a. In fact, comparing the cases of bonding on both faces, the thinnest disc actually deflected a greater absolute distance than did the next thicker disc, though the latter disc was 50% thicker and had a much higher shape factor. Gent & Lindley(see section on bulk compressibility, 1.3.4.2) did predict and observe an eventual leveling

off of S_a with increasing shape factor, but not this decrease in S_a. One difference is that the elastomer tested by Gent & Lindley was, with a Young's modulus of about 270 psi, many times softer than Thordon. The compressive behavior of very stiff elastomers like Thordon may be an area deserving further study, which would probably involve the testing of a large number of shape factors.

The cases of one bonded face with one lubricated face- important here because they correspond to lubricated sleeve bearings with bonded linings- were found to be intermediate in stiffness between the double-lubricated and the double-bonded cases, as might be expected. The presence of 30-micron abrasive powder at the interfaces of the thickest disc was almost the equivalent of bonding so far as compressive stiffness was concerned.

Taking the slopes of the homogeneous compression curves at about 3% deflection for the two thicker slabs and at about 10% deflection for the thinnest slab(because these are the points where the curves straighten out after the initial reverse bends near the origins; slopes were not taken exactly at the origins because these initial bends were not predicted by Fig. 1.4) gives an average Young's modulus E of around 50,000 psi for the given rate of loading; G, which should be about 1/3 of E, should therefore be about 17,000 psi. This value of G is far off the range shown in Table(1.1), bringing the shape functions there into some question.

1.5.2 Sleeve Bearings

Fig.(1.12) shows the apparatus that was set up for measuring the static radial deflections of elastomeric sleeve bearings. The top and bottom of the housing were flattened off to provide good surfaces for applying force and for the contact point of a dial gauge. Another dial gauge was placed under the shaft at a point near the bearing to measure the amount of deflection resulting from bending of the shaft and from indentations at the V-blocks; the difference between the two dial readings was taken as the true deflection of the bearing. A tilting compression head was used to compensate for unevenness in the shaft's supports.

Four different Thordon Regular sleeve bearings were tested, with different surface conditions at the bearing surface and in the interference fit between the lining and the housing. Two of the bearings had lining thicknesses of about 1/10th the bore diameter(approximately the thickness suggested in the current brochure of Thomson-Gordon Ltd.) and differed only in their lengths. The other two bearings had lining thicknesses of less than 1/20th the bore diameter and also differed only in their lengths. The bearing clearance(the difference between the bore and the shaft diameter), which affects the concentration of bearing pressure, was relatively the same for all the bearings.

The test results are shown in Figs.(1.13), (1.14), (1.15), & (1.16). σ_p, the "projected-area" stress, is, by

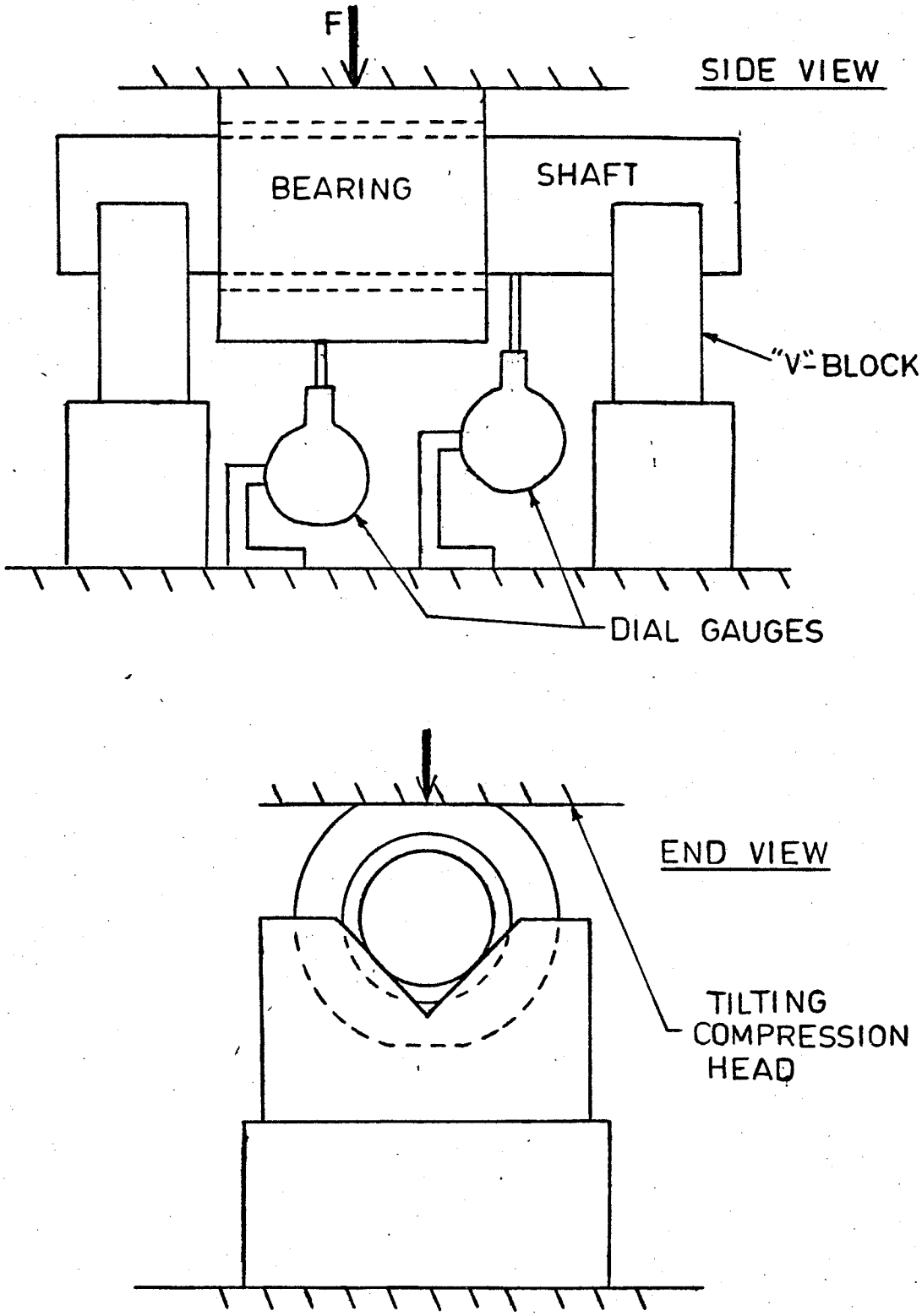

FIG. 1.12 APPARATUS FOR MEASURING STATIC RADIAL DEFLECTIONS OF ELASTOMERIC BEARINGS

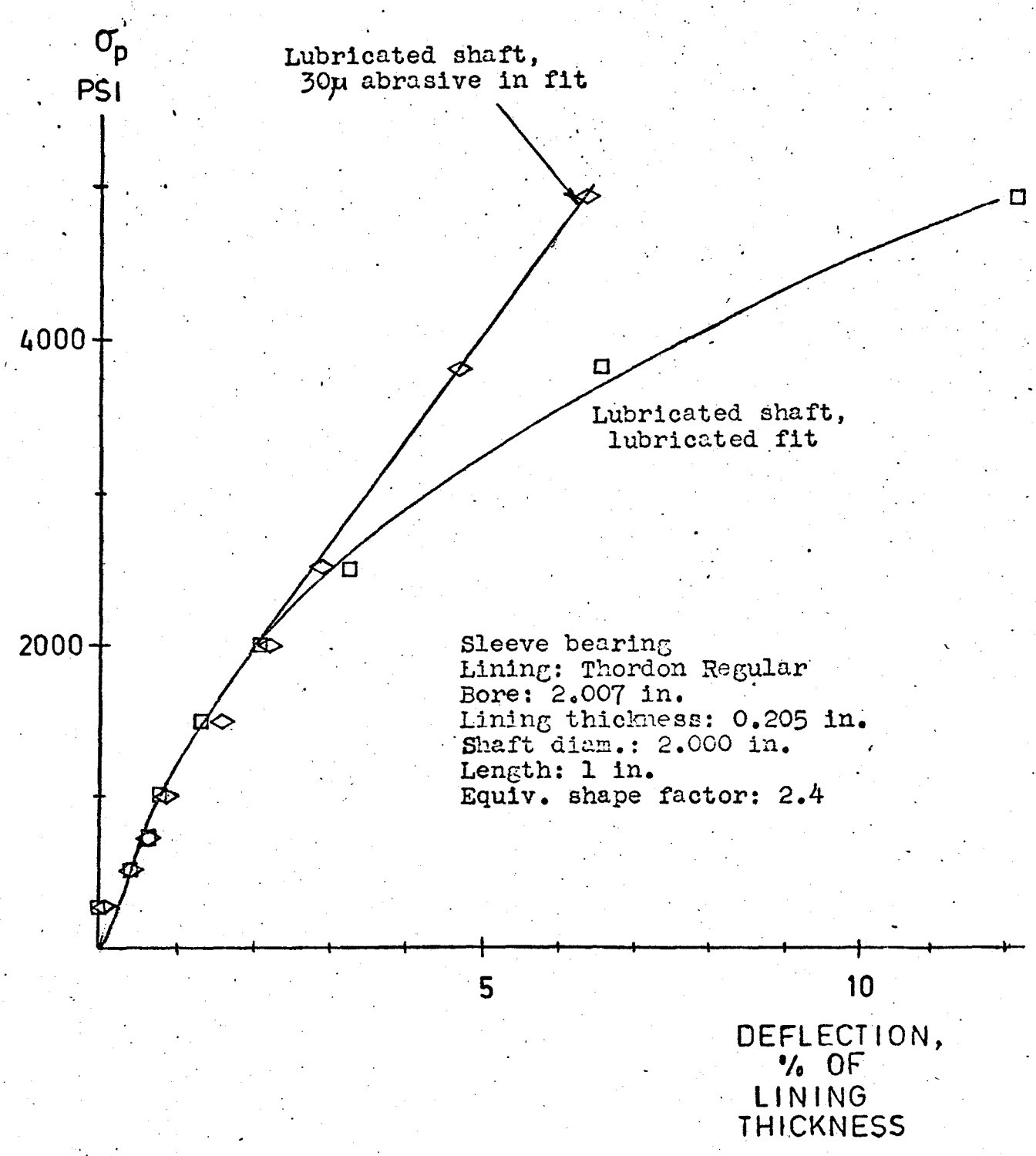
σ_p
PSI
Lubricated shaft,
30μ abrasive in fit
Lubricated shaft,
lubricated fit
4000
2000
Sleeve bearing
Lining: Thordon Regular
Bore: 2.007 in.
Lining thickness: 0.205 in.
Shaft diam.: 2.000 in.
Length: 1 in.
Equiv. shape factor: 2.4
5
10
DEFLECTION,
% OF
LINING
THICKNESS

FIG. 1.13

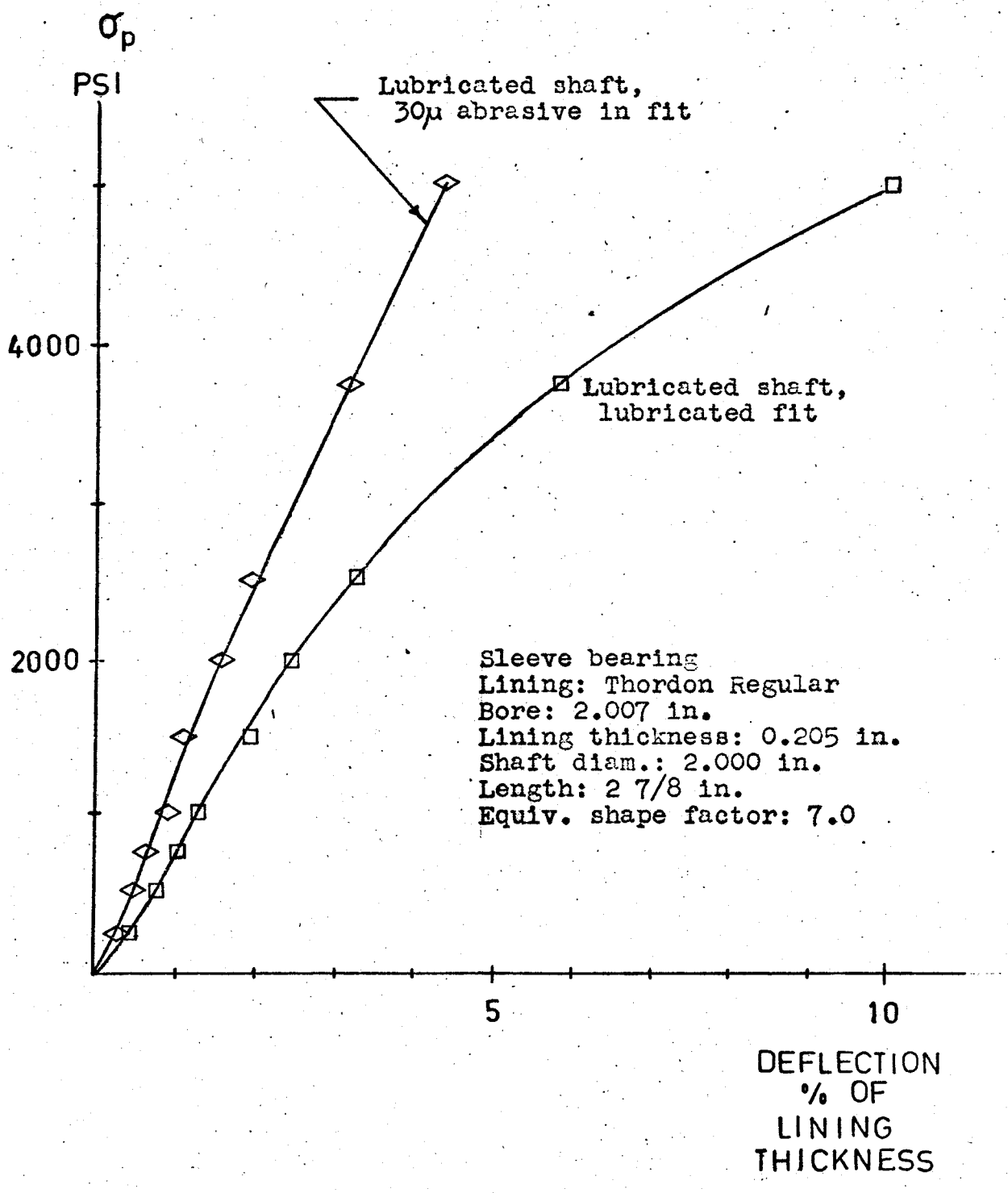
σ_p
PSI
Lubricated shaft,
30μ abrasive in fit
Lubricated shaft,
lubricated fit
4000
2000
Sleeve bearing
Lining: Thordon Regular
Bore: 2.007 in.
Lining thickness: 0.205 in.
Shaft diam.: 2.000 in.
Length: 2 7/8 in.
Equiv. shape factor: 7.0
5
10
DEFLECTION
% OF
LINING
THICKNESS

FIG. 1.14

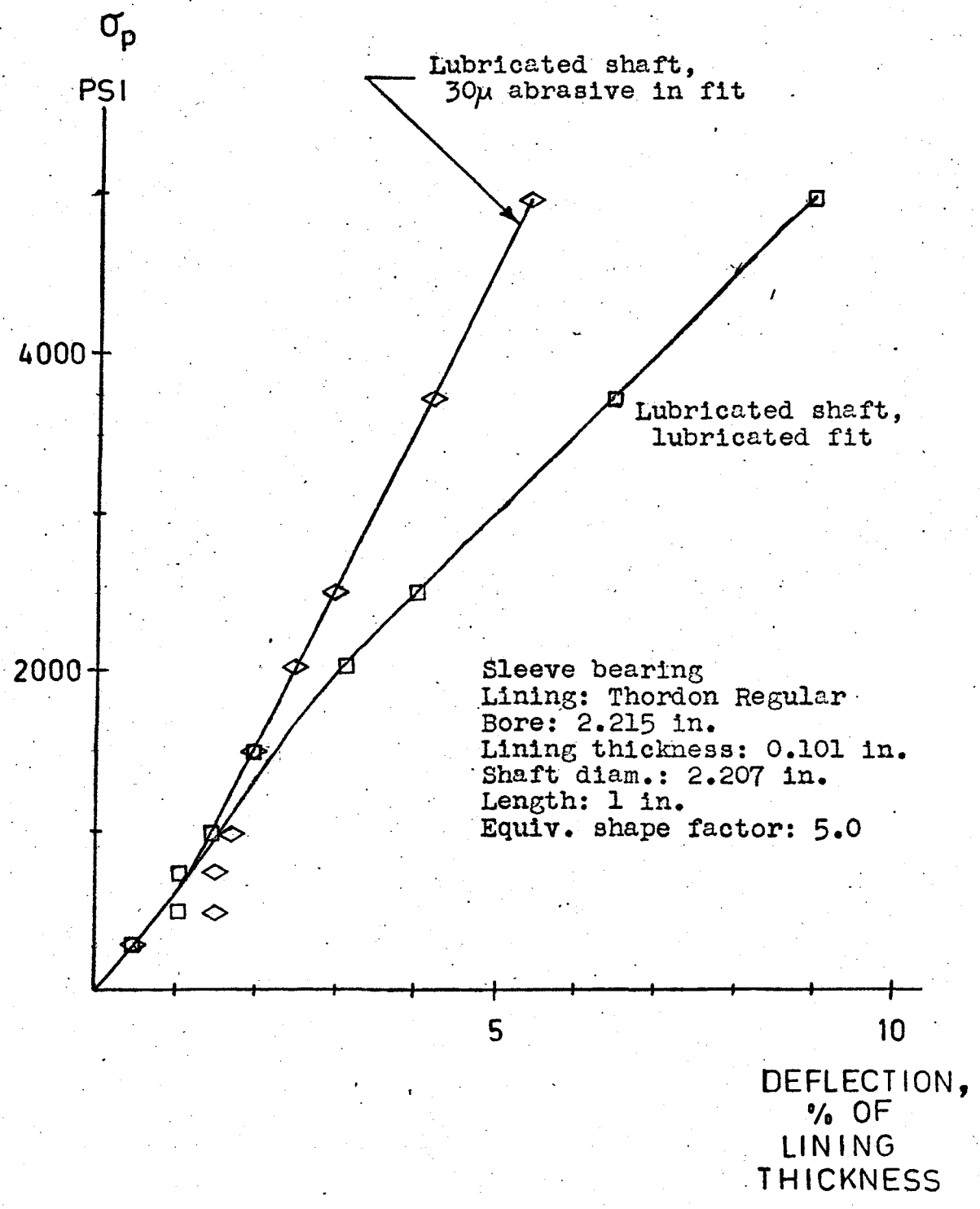
σ_p
PSI
Lubricated shaft,
30μ abrasive in fit
Lubricated shaft,
lubricated fit
4000
2000
Sleeve bearing
Lining: Thordon Regular
Bore: 2.215 in.
Lining thickness: 0.101 in.
Shaft diam.: 2.207 in.
Length: 1 in.
Equiv. shape factor: 5.0
5
10
DEFLECTION,
% OF
LINING
THICKNESS

FIG. 1.15

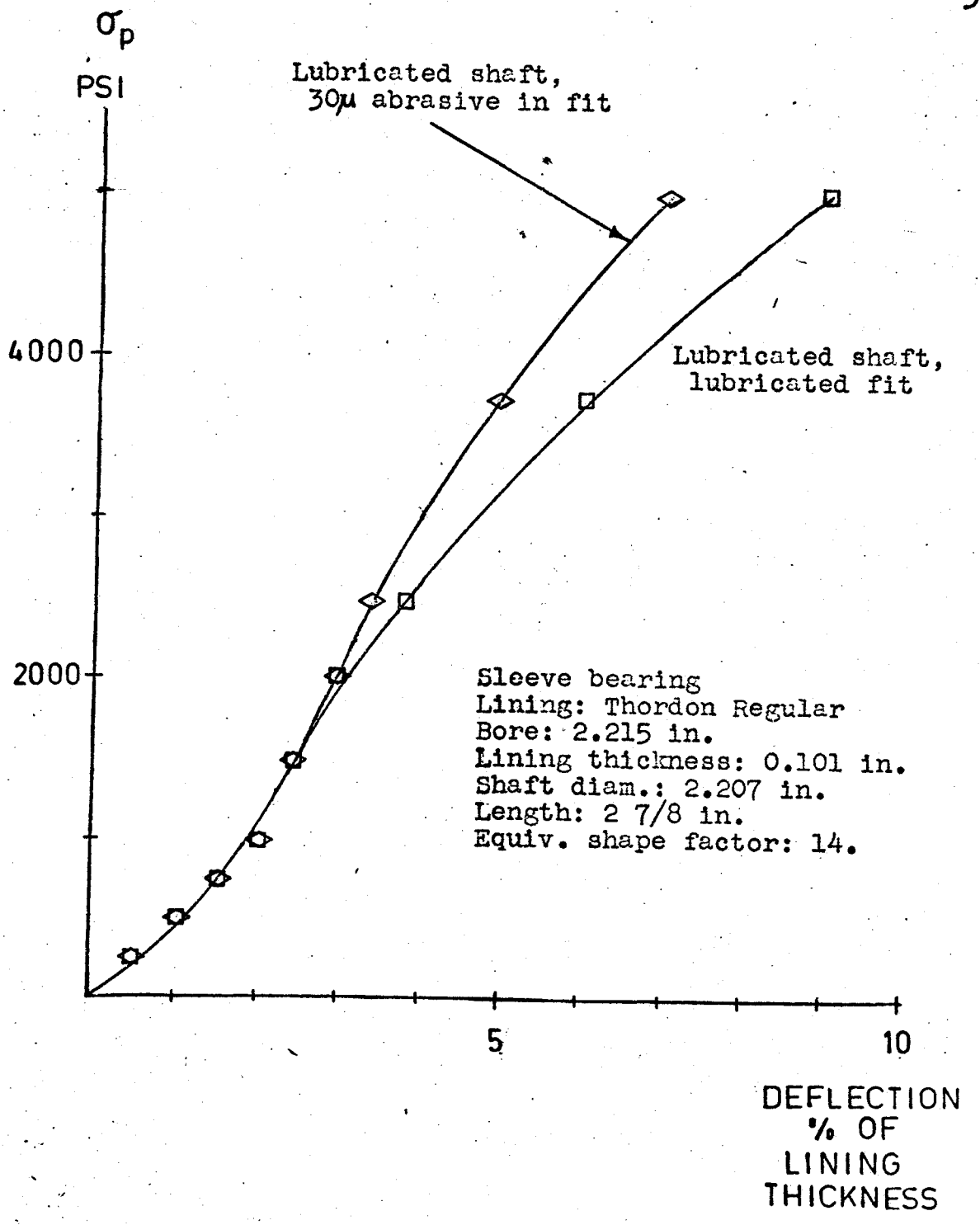
σ_p
PSI
Lubricated shaft,
30μ abrasive in fit
Lubricated shaft,
lubricated fit
4000
2000
Sleeve bearing
Lining: Thordon Regular
Bore: 2.215 in.
Lining thickness: 0.101 in.
Shaft diam.: 2.207 in.
Length: 2 7/8 in.
Equiv. shape factor: 14.
5
10
DEFLECTION
% OF
LINING
THICKNESS

FIG. 1.16

the analogy of Sec.(1.4), here considered to be roughly equivalent to σ in the graphs for the discs. The "equivalent" shape factors are based on Eq.(1.19). When testing, stress was increased in the following jumps, with a pause of about 10 seconds at each level for taking measurements: 250, 500, 750, 1000, 1500, 2000, 2500, 3750, & 5000 psi. This sequence differs slightly from that used in the testing of the discs, but that difference is not significant here. As in the case of the discs, the curves were smoothed by eye through data points that were averages of two tests. Because of Thordon's creep, deflections for slower rates of loading would be somewhat greater.

The purpose of testing the case of a lubricated fit with a lubricated shaft was to provide a comparison with the homogeneous compression of the slabs; it is recommended that in actual practice the interference fit not be lubricated because lubrication there would greatly increase the danger of the lining shifting in the housing(see Sec. 3.1). Note that, like the curves for the homogeneous compressions of the discs, all the curves for the lubricated fit-lubricated shaft condition are similar despite the great differences in bearing geometries. Also, according to the graphs, the bearings appear to be somewhat stiffer in this double-lubricated condition than the discs; this is possibly due to the fact that the bearing linings have their surface slippage restricted in the circumferential direction whereas the discs' surfaces are free

to slip in all directions.

30-micron abrasive powder, spread over cleaned surfaces before press-fitting of the lining, was used to increase the friction between the lining and the housing. Tests with the discs showed the abrasive to be less effective than a bond, but bonding was not tried in the bearings for fear that it would prevent the successful separation and reuse of the lining and the housing. As in the case of the discs, this reduction or elimination of slippage on one face had the effect of increasing the stiffness. Among the bearings, this increase in stiffness was poorest for the bearing with the highest equivalent shape factor(Fig. 1.16), in agreement with the discs, among which the increase was least for the one with the highest shape factor(Fig. 1.11). The probable reason for this correlation is that the shape factors of the discs are comparable in value to the equivalent shape factors of the bearings.

1.6 CONCLUSIONS

Using Figs.(1.9), (1.10), (1.11), (1.13), (1.14), (1.15), & (1.16), the following general conclusions are reached here concerning the radial stiffnesses of the bearings:

(1) In terms of the projected-area stresses and of deflections taken as a percentage of the lining thickness, sleeve bearings of widely differing geometries were found to have similar stress-deflection curves.

(2) Those stress-deflection curves were found to be only somewhat stiffer than those for homogeneous compressions of flat slabs, including the condition of lubrication both on the bearing surface and in the interference fit(though it should again be emphasized that the fit should not be lubricated in practice). This implies that a rough idea of the radial stiffnesses of sleeve bearings of different geometries could be obtained from the homogeneous compression of a single flat slab.

(3) The absolute stiffness of the bearing can generally be improved in the following two ways: (a) by increasing friction, or by bonding, at the interference fit; (b) by reduction of lining thickness. However, (a) provides no significant improvement for Thordon at low bearing pressures and bonding in particular may be expected to increase thermal and liquid-swell bore contractions.

(4) The main benefits from the analogy between sleeve bearings and slabs were that it led to or explained the conclusions above.

(5) The tests on Thordon bearings confirmed the original design estimate of a deflection of about 4% of the wall thickness at a projected-area stress of 2500 psi, provided that this stress is gradually reached in about 1 minute and then released. Because of creep, the deflections for continuous loading periods of hours or days would be substantially greater.

2. CLEARANCES

2.1 INTRODUCTION

In the first part of this thesis, it was shown that for Thordon the radial deflections due to load are generally under 4% of wall thickness when the projected-area pressure is within the recommended operating range of 2,500 psi. On the other hand, the recommended clearance between the bore and the shaft is generally at least 4-5% of wall thickness and even greater where thermal and liquid-swell bore contractions must be allowed for. It is apparent, then, that from the standpoint of accurate shaft alignment, the problem of clearance can be at least as serious as that of elastic deflections- much more serious, in fact, in low pressure, high velocity applications, where deflections are low but heat buildup great.

The term total clearance here means the difference between the diameters of the shaft and the bearing bore at the time of installation. This total clearance might be considered to consist of the following three parts:

(1) Running clearance- the actual clearance required when running to insure smooth operation;

(2) Thermal clearance- allows for thermal expansion of the lining thickness;

(3) Swelling clearance- allows for the swelling caused

by liquids.

Ideally, the last two clearances should be such that the proper running clearance is reached under steady state operation. These three clearances are all contained in the following design equation recommended by a manufacturer[21]:

$$c = 0.004d + 6w(\alpha \Delta T + g) \tag{2.1}$$

The above equation can be broken down as follows:

$0.004d$ = running clearance
$6w\alpha\Delta T$ = thermal clearance
$6wg$ = swelling clearance

where-

c = total clearance
d = bore diameter
w = lining thickness
α = coefficient of thermal expansion
g = relative dimensional changes resulting from effect of liquid absorption
ΔT = difference between temperature on installation and operating temperature (location of latter temperature not specified; presumably it refers to either the bearing surface temperature or the average lining temperature)

No theoretical development was given for Eq.(2.1). The main purpose of this second chapter is to theoretically predict the required thermal and swelling clearances to construct a total clearance equation similar to Eq.(2.1). The running clearance recommendation, however, will be based on those of manufacturers, which are determined from practical experience. Some experimental measurements of the thermal clearance will also be provided.

2.2 RUNNING CLEARANCE

The running clearance should not be so small that seizure results, nor be so great that poor alignment, vibration, and high load concentrations become problems. However, as seizure is the most likely of these factors to cause rapid failure of the bearing, it is better, so far as bearing life is concerned, to err on the high side rather than on the low. For this reason, thermal clearances and swelling clearances should be sufficiently generous to insure that the actual running clearance will remain above the minimum recommended value.

Three different running clearance recommendations, as a function of bore diameter, are shown in Fig.(2.1). One of these(BASF) is based on Eq.(2.1). A safe allowance covering all of them is 0.005d.

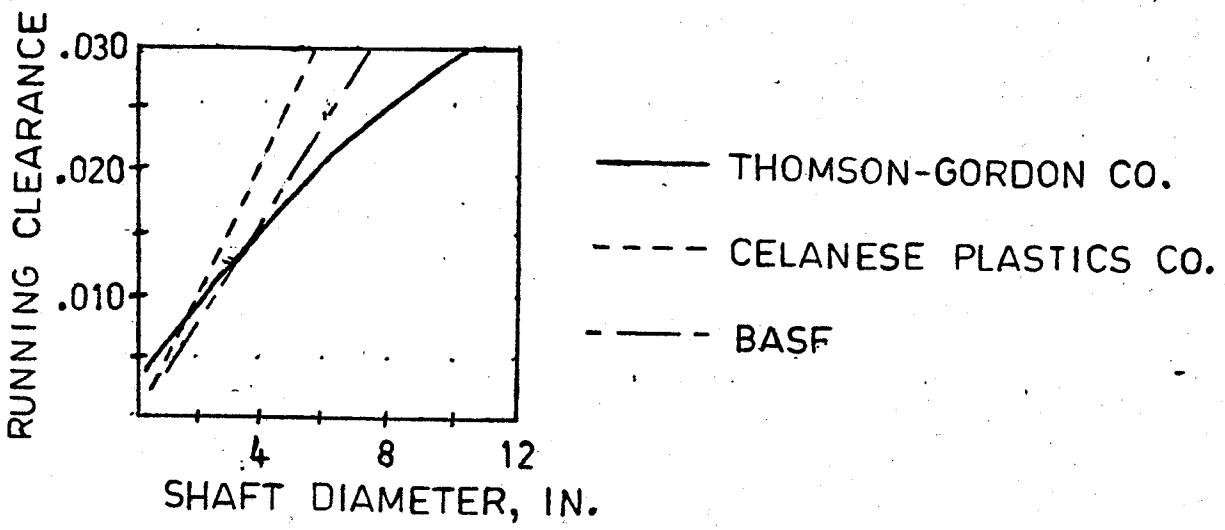

FIG. 2.1 RECOMMENDED RUNNING CLEARANCES

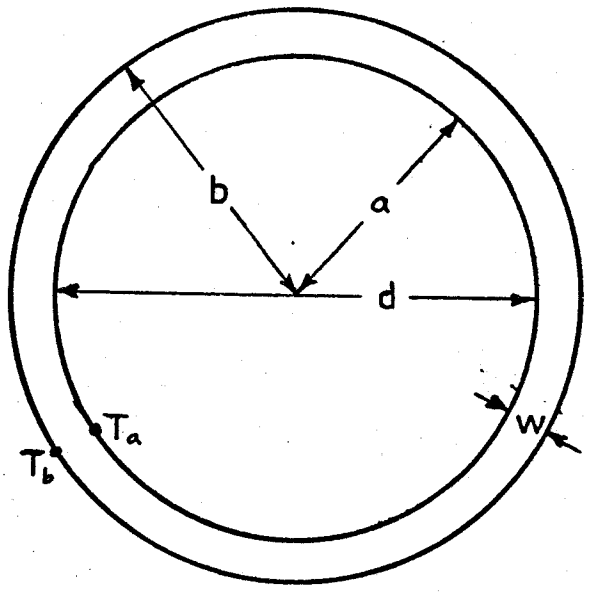

FIG. 2.2 CROSS-SECTION OF LINING

2.3 THERMAL CLEARANCE

2.3.1 Basic Assumptions

There are two ways in which thermal expansions can alter the bearing clearance: (1) by a change in the lining thickness; (2) by a difference between the thermal expansion of the housing and that of the shaft. Despite the fact that metals in general have much lower coefficients of thermal expansion than do elastomers(e.g., $0.7X10^{-5}$in./in.-^{o}F for steel, $1.1X10^{-5}$ for brass, and $1.4X10^{-5}$ for aluminum, vs. about $7X10^{-5}$ in./in.-^{o}F for Thordon, $4X10^{-5}$ for ebonite, and $10X10^{-5}$ to $20X10^{-5}$ for soft rubbers),[22] the individual expansions of the shaft and of the housing can be significant compared to the change in lining thickness; however, the difference between the housing's and the shaft's expansions should be insignificant, provided that the shaft and the housing have comparable coefficients of thermal expansion and do not differ much in operating temperature(an example is included at the end of Sec. 2.3.4). For this reason, the metallic expansions are disregarded here.

Disregarding the metallic expansions, the decrease- or increase, in the case of certain low temperature applications- of the bearing clearance becomes twice the thermal change in wall thickness of the elastomeric lining. This change in wall thickness is estimated here to be the same

as that of an unhoused lining, that is, a lining with no restriction on radial expansion. The basis of this assumption, confirmed by actual measurements, is that the total wall thickness does not change significantly when the lining is pressed into the housing; hence, it should make little difference whether the thermal wall thickness changes are measured with the lining housed or not. In other words, the principle of the superposition of mechanical and thermal strains is assumed to hold. The following additional assumptions and techniques are used here:

(1) The temperature distribution in the lining is assumed to be independent of the axial coordinate z; this assumption seems justified by the high length to wall-thickness ratio, which should minimize end effects.

(2) The temperature distribution is assumed to be symmetrical about the axis; this assumption may not be completely valid where the temperature buildup concentrates on the loaded side of the bearing, but greatly simplifies the problem and may be expected to give a conservative answer.

(3) There is a condition of steady heat flow.

(4) It was found to be easier in this problem to treat the total thermal deformation of the unhoused lining as a superposition of the following two imaginary stages: (a) a uniform temperature rise- that deformation which would occur

by the uniform temperature change of the entire lining(Fig. 2.2) from T_o, the installation temperature, to T_b, the operating temperature of the lining's outer radius(this includes those low temperature applications where T_b is less than T_o); (b) the addition of the nonuniform temperature field- that further deformation which would result from then raising the inner radius to its operationg temperature, T_a, while holding the outer radius at T_b. This superposition is valid because the radial displacement u is linear with T in Eq.(2.2) and can also be shown to be so in Eq.(2.29).

(5) The thermal conductivity and the coefficient of thermal expansion are assumed to be temperature-independent.

(6) The solution selected will be that for plane strain with e_z=0(i.e., plane strain with zero axial strain). e_z=0 was chosen because it is desired here to allow for the worst situation and it is intuitively apparent that the thermal bore contraction would be more severe where the lining is axially constrained by bonding or friction in the housing fit than where the lining is free to expand axially as in a well-lubricated fit. Unfortunately, however, the available solutions are for the case of F_z=0 (plane strain with zero end force), that is, where a uniform axial stress, such as to make the cylinder's end faces free of axial forces, is superposed on the axial stress for e_z=0. Therefore, the solution for e_z=0 will be derived from that for F_z=0 by a

formula developed here to effect the conversion.

(7) For plane strain with $e_z=0$, it is only necessary to assume that all cross-sections are in the same condition of thermoelasticity; it is not necessary to assume, as in the case of plane strain with $F_z=0$, that the cylinder is very long and that the uncorrected solution is valid only far away from the ends(this is because the solution for $F_z=0$ does not satisfy the boundary conditions at the ends; there must therefore be self-equilibrating end effects which, by Saint Venant's principle, become negligible at a sufficient distance from the ends).

(8) A thin-wall approximation is assumed for the case of the nonuniform temperature field.

(9) For generality, the shaft's and housing's expansions, previously assumed to be equal, are here assumed to both be zero. This new assumption makes no difference so far as the clearance is concerned. The amount of bore contraction then corresponds to the thermal clearance and becomes equal to twice the change in lining thickness.

2.3.2 Solution for Zero End Force

2.3.2.1 Radial Displacements for Unhoused Lining

(a) General

For plane strain with $F_z=0$, the radial displacements in a long cylinder at a distance far from the ends is[23] in the absence of external stresses:

$$(2.2)\quad u_f(r) = \frac{\alpha}{r(1-\nu)}\left((1+\nu)\int_a^r Tr\,dr + \frac{(1-3\nu)r^2+a^2(1+\nu)}{b^2-a^2}\int_a^b Tr\,dr \right)$$

-where u and T are relative to what is considered the equilibrium condition; that is,

$u_f(r)$ = radial displacement of a point at radius r (as this equation is for small strains, it does not matter whether this r is considered initial or final), relative to that point's position in what is considered the unheated (i.e., T=0 everywhere; see definition of T below) condition of the cylinder. The subscript f refers to the condition $F_z=0$.

$T = T(r)$ = temperature distribution, here a function of the radius r, in an arbitrary temperature scale in which T=0 everywhere corresponds to u=0 everywhere.

α = coefficient of thermal expansion

a = inner radius of cylinder

b = outer radius of cylinder

ν = Poisson's ratio

For the inner radius a and the outer radius b, Eq.(2.2) reduces to:

$$(2.3)\quad u_f(a) = \frac{2\alpha a}{b^2-a^2}\int_a^b Tr\,dr$$

$$(2.4)\quad u_f(b) = \frac{2\alpha b}{b^2-a^2}\int_a^b Tr\,dr$$

(b) Uniform Temperature Change

The radial displacements for a uniform temperature change of the entire lining(here regarded as unhoused) from T_o, the installation temperature, to T_b, the operating temperature of the lining's outer radius, are, from Eqs. (2.3) and (2.4),

$$(2.5) \quad u_{fu}(a) = \frac{2\alpha a}{b^2-a^2} \int_a^b (T_b-T_o)r\,dr = \alpha a(T_b-T_o)$$

Similarly,

$$(2.6) \quad u_{fu}(b) = \alpha b(T_b-T_o)$$

-where the subscript u refers to the uniform temperature change.

(c) Nonuniform Temperature Field

Though this case can be solved by substituting the temperature distribution into Eqs.(2.3) and (2.4), another approach that is simpler because the stresses are known will be used here. The development up to Eq.(2.10) does not involve the assumption of zero end force.

Due to the assumption of an axially symmetric temperature distribution, there are no tangential displacements; the tangential strain e_θ therefore reduces to:[24]

$$(2.7) \quad e_\theta = \frac{u}{r}$$

Hooke's Law, modified to include thermal strains, gives:[25]

$$(2.8) \qquad e_\theta = \frac{1}{E}(\sigma_\theta - \nu(\sigma_r+\sigma_z)) + \alpha T$$

Combining Eqs.(2.7) and (2.8) gives:

$$(2.9) \qquad u = r\left(\frac{1}{E}(\sigma_\theta - \nu(\sigma_r+\sigma_z)) + \alpha T \right)$$

Eq.(2.9) is an alternate expression to Eq.(2.2) but is not restricted to the case $F_z=0$.

Now, the obvious boundary conditions for the inner radius a and the outer radius b are:

$$(2.10) \qquad \sigma_r(a) = \sigma_r(b) = 0$$

Also, provided that the following conditions are met,

(1) There is steady heat transfer with temperatures of T_a on the inner radius and T_b on the outer radius.

(2) A uniform temperature of T_b is taken as the unstrained condition.

(3) $F_z = 0$

(4) A thin wall approximation is made.

-then the other stresses at a and b reduce to:[26]

$$(2.11) \qquad \sigma_{\theta f}(a) = \sigma_{zf}(a) = -\frac{\alpha E(T_a - T_b)}{2(1-\nu)}$$

$$(2.12) \qquad \sigma_{\theta f}(b) = \sigma_{zf}(b) = \frac{\alpha E(T_a - T_b)}{2(1-\nu)}$$

-where the subscript f again refers to the condition $F_z=0$.

Substituting Eqs.(2.10), (2.11), and (2.12) into Eq.(2.9), with, in Eq.(2.9), $T=T_a-T_b$ for r=a and T=0 for r=b (the respective temperature rises at these two radii, referred to T_b) gives:

$$(2.13)\qquad u_{fn}(a) = \tfrac{1}{2}\alpha a(T_a-T_b)$$
$$u_{fn}(b) = \tfrac{1}{2}\alpha b(T_a-T_b)$$

-where the subscript n refers to the nonuniform temperature field.

(d) Combined Displacement

Combining Eqs.(2.5), (2.6), and (2.13) gives the following total displacements:

$$(2.14)\quad u_f(a) = u_{fn}(a) + u_{fu}(a) = \alpha a(\tfrac{1}{2}(T_a+T_b)-T_o)$$

$$(2.15)\quad u_f(b) = u_{fn}(b) + u_{fu}(b) = \alpha b(\tfrac{1}{2}(T_a+T_b)-T_o)$$

2.3.2.2 Changes in Lining Thickness and Bore Diameter

If (Δw) denotes the change in thickness for the unhoused lining(or for the housed lining, by the assumption of no change in w during press-fitting), then:

$$(2.16)\quad (\Delta w)_f = u_f(b) - u_f(a)$$

From Eqs.(2.14) and (2.15), Eq.(2.16) becomes:

$$(2.17)\quad (\Delta w)_f = (b-a)\alpha(\tfrac{1}{2}(T_a+T_b)-T_o)$$

-or, since (b-a)=w, Eq.(2.17) can be written,

$$(2.18)\quad (\Delta w)_f = w\alpha(\tfrac{1}{2}(T_a+T_b)-T_o)$$

By the assumption of zero housing expansion, the bore

change, denoted below by Δd, is the negative of twice the change in lining thickness; that is,

$$(\Delta d)_f = -2(\Delta w)_f$$

Eq.(2.18) then gives:

$$(2.19) \qquad (\Delta d)_f = -2w\alpha\left(\tfrac{1}{2}(T_a+T_b)-T_o\right)$$

-where, in summary,

Δd = change in bore diameter between installation and steady state operation
w = lining thickness
α = coefficient of thermal expansion
T_a = operating temperature of inner radius of lining
T_b = operating temperature of outer radius of lining
T_o = installation temperature(or any other uniform temperature at which Δd is considered to be zero)

-and where it should be noted that

$\left(\tfrac{1}{2}(T_a+T_b)-T_o\right)$ = "average" operating temperature in lining (for a thin wall, the temperature distribution is nearly linear and this can therefore be taken as the true average) minus the installation temperature

Eq.(2.19) predicts a bore contraction when the average operating temperature is greater than T_o, and a bore expansion when it is less.

Eq.(2.19) is for $F_z=0$, whereas the desired solution, to be developed next, is for $e_z=0$. However, Eq.(2.19) is to be used later for comparison.

2.3.3 Solution for Zero Axial Strain

2.3.3.1 Radial Displacements for Unhoused Lining

(a) Conversion of solutions- obtaining solution for $e_z=0$ from that for $F_z=0$.

Eq.(2.9) is still valid here; that is,

$$u_e = r\left(\frac{1}{E}(\sigma_{\theta e}-\nu(\sigma_{re}+\sigma_{ze})) + \alpha T\right) \tag{2.20}$$

-where the subscript e denotes the condition $e_z=0$.

For the same temperature distribution, σ_r and σ_θ are unchanged[27] from the case of $F_z=0$; that is,

$$\sigma_{re} = \sigma_{rf} \quad \text{and} \quad \sigma_{\theta e} = \sigma_{\theta f} \tag{2.21}$$

From (2.21), (2.20) may be written,

$$u_e = r\left(\frac{1}{E}(\sigma_{\theta f}-\nu(\sigma_{rf}+\sigma_{ze})) + \alpha T\right) \tag{2.22}$$

-where the right side of Eq.(2.22) is the same as the solution for $F_z=0$ except for the term σ_{ze}; hence, the difference between the two cases is entirely due to their difference in the term σ_z.

Now, the following two relations hold[28] for σ_z:

$$\sigma_{ze} = \nu(\sigma_{re}+\sigma_{\theta e}) - \alpha E T \tag{2.23}$$

and

$$\sigma_{zf} = \sigma_{rf}+\sigma_{\theta f} \tag{2.24}$$

From Eqs.(2.21) and (2.24), Eq.(2.23) can be written,

$$\sigma_{ze} = \nu(\sigma_{rf}+\sigma_{\theta f}) - \alpha E T = \nu(\sigma_{zf}) - \alpha E T \tag{2.25}$$

Substituting Eq.(2.25) into Eq.(2.22) gives the

following:

$$(2.26) \qquad u_e = r\left(\frac{1}{E}(\sigma_{\theta f} - \nu(\sigma_{rf} + \nu(\sigma_{zf}) - \alpha E T)) + \alpha T \right)$$

Rewriting Eq.(2.26),

$$(2.27) \qquad u_e = r\left(\frac{1}{E}(\sigma_{\theta f} - \nu(\sigma_{rf} + \sigma_{zf} - (1-\nu)\sigma_{zf} - \alpha E T)) + \alpha T \right)$$

Removing the terms $(1-\nu)\sigma_{zf}$ and $\alpha E T$ from inside the inner parenthesis gives:

$$(2.28) \qquad u_e = r\left(\frac{1}{E}(\sigma_{\theta f} - \nu(\sigma_{rf} + \sigma_{zf})) + \alpha T \right) + r\frac{\nu}{E}((1-\nu)\sigma_{zf} + \alpha E T)$$

Of the two large terms on the right hand side of Eq.(2.28), the first is, by Eq.(2.9), merely the solution for $F_z = 0$; therefore,

$$(2.29) \qquad u_e = u_f + r\frac{\nu}{E}((1-\nu)\sigma_{zf} + \alpha E T)$$

Hence, according to Eq.(2.29), u_e can be found simply by adding the given expression to u_f, assuming, of course, that the same temperature distribution exists.

(b) Uniform Temperature Change

Before applying Eq.(2.29), it will first be shown that σ_{zf} is zero for a uniform temperature change.

From Timoshenko and Goodier,[29]

$$(2.30) \qquad \sigma_{rf} = \frac{\alpha E}{(1-\nu)} \frac{1}{r^2}\left(\frac{r^2-a^2}{b^2-a^2} \int_a^b Tr\, dr - \int_a^r Tr\, dr\right)$$

and

$$(2.31)\quad \sigma_{\theta f} = \frac{\alpha E}{(1-\nu)}\frac{1}{r^2}\left(\frac{r^2+a^2}{b^2-a^2}\int_a^b Tr\,dr + \int_a^r Tr\,dr - Tr^2\right)$$

For a uniform temperature change(T constant, regardless of r), Eqs.(2.30) & (2.31) reduce to:

$$(2.32)\quad \sigma_{rf} = \sigma_{\theta f} = 0$$

Eqs.(2.24) and (2.32) then give:

$$(2.33)\quad \sigma_{zf} = 0$$

Now applying Eq.(2.29) with Eqs.(2.5), (2.6) and (2.33) gives:

$$(2.34)\quad u_{eu}(a) = \alpha a(T_b-T_o)+a\frac{\nu}{E}(\alpha E(T_b-T_o)) = (1+\nu)\alpha a(T_b-T_o)$$

and:

$$(2.35)\quad u_{eu}(b) = (1+\nu)\alpha b(T_b-T_o)$$

-where the subscript u again denotes the uniform temperature change. The radial displacements here differ by a factor of $(1+\nu)$ from the corresponding ones for $F_z=0$, Eqs.(2.5) & (2.6).

(c) Nonuniform Temperature Field

Applying Eq.(2.29) with Eqs.(2.11) and (2.13) gives:

$$u_{en}(a) = \tfrac{1}{2}a\alpha(T_a-T_b) + a\frac{\nu}{E}\left((1-\nu)\left(-\frac{\alpha E(T_a-T_b)}{2(1-\nu)}\right) + \alpha E(T_a-T_b)\right)$$

or, simplifying,

$$(2.36)\quad u_{en}(a) = \tfrac{1}{2}(1+\nu)\alpha a(T_a-T_b)$$

-where the subscript n again denotes the nonuniform temperature field.

Similarly, from Eq.(2.29) (with T=0, the temperature change at radius b during the introduction of the nonuniform temperature field) and Eqs.(2.12) & (2.13),

$$u_{en}(b) = \tfrac{1}{2}b\alpha(T_a-T_b) + b\frac{\nu}{E}\left((1-\nu)\left(\frac{\alpha E(T_a-T_b)}{2(1-\nu)}\right) \right)$$

or

$$u_{en}(b) = \tfrac{1}{2}(1+\nu)\alpha b(T_a-T_b) \tag{2.37}$$

(d) Combined Displacement

Combining Eqs.(2.34) through (2.37) gives the following total displacements:

$$u_e(a) = u_{eu}(a) + u_{en}(a)$$

or

$$u_e(a) = (1+\nu)\alpha a(\tfrac{1}{2}(T_a+T_b)-T_o) \tag{2.38}$$

$$u_e(b) = u_{eu}(b) + u_{en}(b)$$

or

$$u_e(b) = (1+\nu)\alpha b(\tfrac{1}{2}(T_a+T_b)-T_o) \tag{2.39}$$

2.3.3.2 Changes in Lining Thickness and Bore Diameter

As for the case of $F_z=0$,

$$(\Delta d)_e = -2(\Delta w)_e = -2(u_e(b)-u_e(a)) \tag{2.40}$$

From Eqs.(2.38) and (2.39), Eq.(2.40) becomes, with $w = b-a$,

$$(\Delta d)_e = -2(1+\nu)w\alpha(\tfrac{1}{2}(T_a+T_b)-T_o) \tag{2.41}$$

The solution here differs by a factor of $(1+\nu)$ from that for $F_z=0$, Eq.(2.19), as does each of the displacements derived above.

Letting $\nu = \frac{1}{2}$, for elastomers, Eq.(2.41) becomes

(2.42) $$(\Delta d)_e = -3w\alpha(\tfrac{1}{2}(T_a+T_b)-T_o)$$

Eq.(2.42) is the solution for the assumed condition of $e_z=0$. Eq.(2.42), like Eq.(2.19), predicts a bore contraction when the average lining temperature is greater than T_o, the installation temperature, and a bore expansion when it is less.

2.3.4 Experimental Measurement(including temperatures)

The apparatus shown in Fig.(2.3) was used to measure the actual temperatures and bore contractions in a heated Thordon sleeve bearing. SAE 50 motor oil was selected as the heating medium in preference to water for the following reasons:

(1) The higher temperatures attainable;

(2) Thordon swells in water but is not supposed to swell or deteriorate in oil;

(3) -to protect the measuring instruments.

However, the fire hazard from the oil required caution..

The bore diameter was measured with a telescopic bore gauge and a micrometer. The temperatures were measured with copper-constantan thermocouples inserted at the points shown. Measurements were taken to the nearest .001 in. at oil temperature levels of 150 ^{o}F, 200 ^{o}F, and 250 ^{o}F, after waiting a few minutes at each level for thermal equilibrium to be reached. Both a standard(recommended) lining thickness and a half-standard thickness were tested. The results,

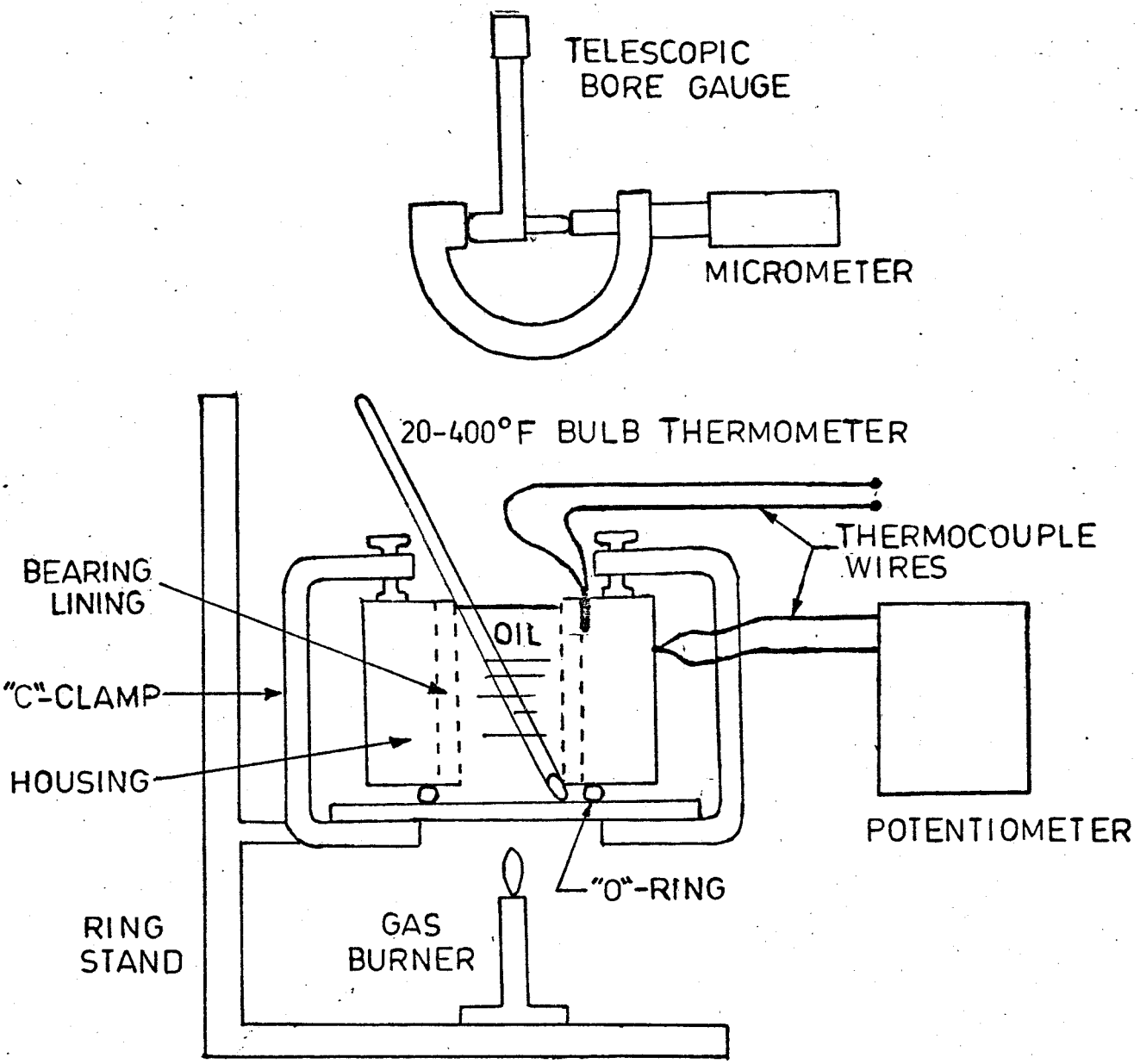

APPARATUS FOR MEASURING THE THERMAL BORE CONTRACTION AND THE TEMPERATURES IN ELASTOMER- AND PLASTIC-LINED SLEEVE BEARINGS

FIG. 2.3

as corrected to compensate for the thermal expansion of the housing, are shown in Fig.(2.4). T_s refers to the temperature of the outer surface of the housing. Both the installation temperature T_o and the ambient temperature during testing were 77 ^{o}F.

A special word should be said about the proper technique for the accurate dimensional measurement of elastomeric articles. The problem is that the tendency of the material to deflect under the measuring instrument can lead to errors of several thousandths of an inch. This is particularly serious where the measurements are made on an unhoused lining, as then the entire lining can warp out of shape(for this reason, it is best to measure bores when the lining is in the housing); however, it is a problem with housed linings as well. An improved method, employed here, is to use the measuring instrument like a feeler gauge, starting with a slightly loose adjustment(undersize for inside diameters, oversize for outside diameters), changing the setting one-thousandth of an inch at a time(using an outside micrometer to preset the telescopic gauge) and testing each setting by dragging or sliding the instrument across the dimension to be measured; the last setting before a sudden slight increase in drag is felt is then taken as the actual dimension. Unfortunately, this method is highly sensitive to "feel." A still better method would be to take a shaft a few thousandths of an inch undersize(for the

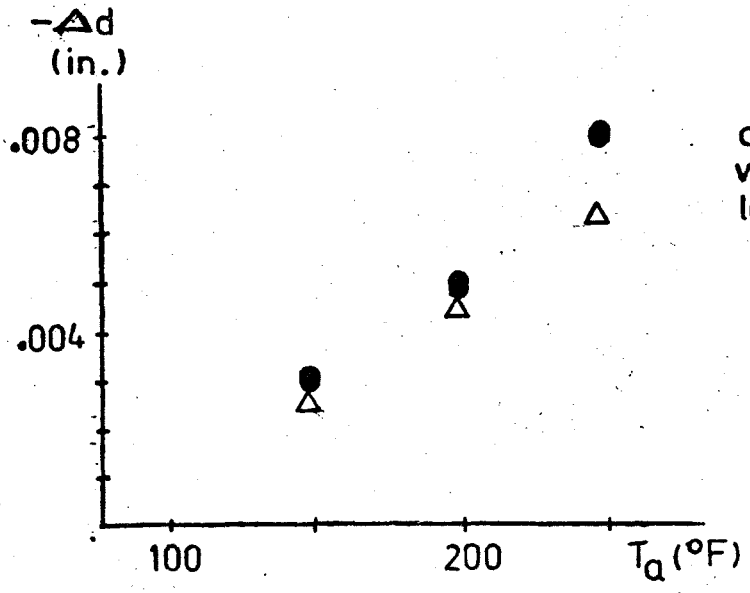

d=2.01"
w=.21"
length=3"

T_a	T_b	T_s	
150	126	120	°F
200	153	149	
250	185	176	

● - MEASURED VALUES

Δ - CALCULATED VALUES - EQ. 2.42

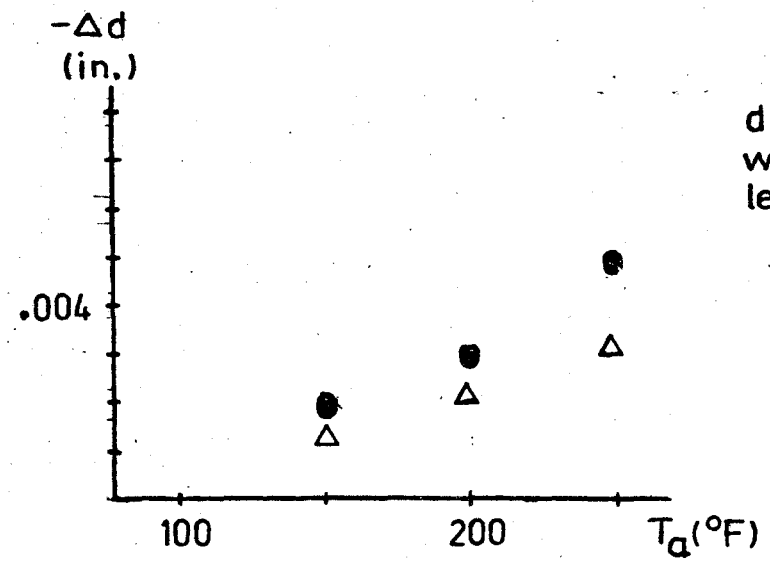

d=2.22"
w=.10"
length=3"

T_a	T_b	T_s	
150	126	118	°F
200	156	149	
250	189	178	

FIG. 2.4 EXPERIMENTAL RESULTS FOR TEMPERATURE DISTRIBUTIONS AND THERMAL BORE CONTRACTIONS (THORDON LININGS)

apparatus of Fig. 2.3, the shaft should be hollow to prevent overflow of the oil) and measure the clearance with a set of leaf-type feeler gauges, the broad surfaces of the feeler gauges reducing the problem of indentation of the material. Perhaps the best method, which unfortunately would require special preparation for each range of measurement, would be to use a set of "go-no-go" fixed diameter cylindrical plug gauges. Whatever method is used, the thermal expansion of the gauge itself should be accounted for. Alternatively, the tests might be made with a lining of a stiffer material of high thermal expansion, though not so stiff as to affect the expansion of the housing.

An example below shows how the corrections for the housing's expansions were made. The housing was a cylindrical steel shell of 2.4 in. inside diameter and 4 in. outside diameter. The expansion of the inside diameter of the shell was taken to be twice the radial change given by Eq.(2.14); that is,

$$(\Delta d)_{shell} = 2\alpha a\left(\tfrac{1}{2}(T_a+T_b)-T_o\right) \qquad (2.43)$$

-where a, b, and d here refer to the dimensions of the shell.

The installation temperature T_o was 77 ^oF; for the oil temperature of 250 ^oF, the "average" shell temperature was about 183 ^oF, and the coefficient of thermal expansion for steel is about $0.7X10^{-5}$ in./in.-^oF; the equation above gives here

(2.44) $(\Delta d)_{shell} = 2(0.7X10^{-5})(1.2)(183-77) = .0018$ in. expansion

This expansion of the shell counteracts the lining's bore contraction, making the amount of the latter smaller than it would be for a truly fixed housing. Hence, since for this oil temperature the measured bore contraction for the standard lining was about .006 in., the bore contraction in a fixed housing would be, according to Eq.(2.44), .006 + .002 = .008 in. All of the measured bore contractions shown in Fig.(2.4) were corrected in this way.

In Fig.(2.4), note that the thinner wall produces considerably lower bore contractions, as predicted by Eq.(2.42). Also, the measurements agree fairly well with the theoretical predictions of Eq.(2.42), which were based on an α of $7X10^{-5}$ in./in.-^{o}F (determined by measuring the expansion of a heated Thordon rod) and on the measured temperatures; most of the discrepancies are within a thousandth of an inch.

If a shaft were also of steel and approximately at the same temperature as the lining bore, its expansion would be, for the standard thickness lining and the bore temperature of 250 ^{o}F,

$$(0.7X10^{-5})(2)(250-77) = .0024 \text{ in. expansion}$$

The difference between this and the housing's expansion, Eq.(2.44), is negligible compared to the lining's expansion for this temperature, thus justifying for this situation the neglect of metallic expansions when theoretically estimating the thermal clearance.

2.3.5 Heat Transfer Considerations

According to Eq.(2.42), the thermal bore change is dependent not only on the operating temperature of the bearing surface, T_a, but also on the operating temperature of the outer radius of the lining, T_b. Unfortunately, these temperatures vary from one application to another and it is usually difficult to predict them even in a given application.

Elastomers in general have very low thermal conductivities, which are comparable, in fact, to those of thermal insulating materials. The thermal conductivity of hard rubber is about 0.09 BTU/hr-ft-^{o}F and that of Thordon is about 0.06, compared to typical values of 10-100 BTU/hr-ft-^{o}F for metals. Hence, by the electrical analogy of heat transfer, where temperature drop corresponds to voltage drop and thermal resistance to electrical resistance, the thermal drop across the lining would be expected to be large compared to that across the metallic housing, even if the lining were quite thin; this expectation is certainly satisfied by the temperature distributions shown in Fig.(2.4). However, because of the thermal resistance between the housing itself and the atmosphere, the thermal drop across the lining is likely to be, as in Fig.(2.4), only a fraction of the total thermal drop between the bearing surface and the atmosphere. Hence, it is assumed for simplicity that the average lining temperature, $\frac{1}{2}(T_a+T_b)$, is practically the same as the bearing

surface temperature. This assumption permits Eq.(2.42) to be written in the same form as the thermal clearance of Eq.(2.1); that is,

(2.45) $$(\Delta d)_e = -3w\alpha\Delta T$$

-where

ΔT = difference between the average lining temperature(or, if desired, the bearing surface temperature) and the temperature at installation. When the former temperature is lower than the latter, the bore should expand safely away from the shaft and hence no thermal clearance should then be required

2.4 SWELLING CLEARANCE

2.4.1 Analogy to Thermoelasticity

The stresses and strains resulting from liquid-swell can be mathematically determined in the same manner as those resulting from thermal expansion if the swelling expansion g is substituted for the thermal expansion αT for each infinitesimal body element. Use of this analogy is made below. It is assumed here, as in the section on thermal deformation, that the bore change is twice what the wall-thickness change of an unhoused lining would be. It is also assumed that the swelling is uniform throughout the lining. Zero axial strain is again assumed; however, the solution for zero end force is also developed for comparison.

2.4.2 Solution for Zero End Force

Substituting g for αT in Eqs.(2.3) and (2.4) gives, for the radial displacements produced in an unhoused lining by swelling,

$$u_{fs}(a) = \frac{2a}{b^2-a^2}\int_a^b gr\,dr \tag{2.46}$$

and

$$u_{fs}(b) = \frac{2b}{b^2-a^2}\int_a^b gr\,dr \tag{2.47}$$

-where the subscript s refers to swelling and the subscript f again refers to the condition $F_z=0$.

For uniform swelling(constant g), Eqs.(2.46) and (2.47) give

(2.48) $u_{fs}(a) = ga$

and

(2.49) $u_{fs}(b) = gb$

The wall thickness change is, using Eqs.(2.48) and (2.49),

(2.50) $(\Delta w)_{fs} = u_{fs}(b)-u_{fs}(a) = g(b-a) = gw$

and the bore contraction is

(2.51) $(\Delta d)_{fs} = -2(\Delta w)_{fs} = -2gw$

2.4.3 Solution for Zero Axial Strain

In the equations of thermoelasticity, uniform swelling corresponds to a uniform temperature rise. The radial displacements for the uniform temperature rise (T_b-T_o) and the condition $e_z=0$ are given by Eqs.(2.34) and (2.35). Substituting g for $\alpha(T_b-T_o)$ in those equations gives

(2.52) $u_{es}(a) = (1+\nu)ga$

and

(2.53) $u_{es}(b) = (1+\nu)gb$

The wall expansion is, from Eqs.(2.52) and (2.53),

(2.54) $(\Delta w)_{es} = u_{es}(b)-u_{es}(a) = (1+\nu)g(b-a) = (1+\nu)gw$

-and, with $\nu=\frac{1}{2}$ for elastomers,

(2.55) $(\Delta d)_{es} = -2(\Delta w)_{es} = -2(1+\nu)gw = -3gw$

Here, as in the case of thermal expansions, the solution for $e_z=0$ is $1\frac{1}{2}$ times as great as that for $F_z=0$, Eq.(2.51).

2.5 CONCLUSION- RECOMMENDED TOTAL CLEARANCE

Combining the running clearance of Sec.(2.2), the thermal clearance of Eq.(2.45), and the swelling clearance of Eq.(2.55) gives

$$c = 0.005d + 3w(\alpha \Delta T + g) \tag{2.56}$$

The symbols above are defined under Eq.(2.1).

The thermal clearance and swelling clearance recommendations of Eq.(2.56) are half those of Eq.(2.1). However, the thermal clearance in Eq.(2.56) is intended to allow only for the lining's expansion; if the shaft is much hotter or has a higher coefficient of thermal expansion than the housing, the estimated difference between the shaft's and the housing's thermal expansions should be added to the clearance given by Eq.(2.56). When in doubt, it is better to increase the clearance, as explained in Sec.(2.2).

3. INTERFERENCE FIT WITH HOUSING

3.1 NORMAL TEMPERATURES

The high friction provided by an interference fit between the lining and the housing is often the only means used for anchoring the lining in place, though, of course, other means, such as bonding, dovetail grooves, or end flanges, might be employed. The purpose of this section is to try to determine the amount of interference necessary to prevent axial or rotary slippage of the lining in the housing. Pure axial slippage might occur in the case of an axially sliding shaft; rotary slippage is undesirable because of wear and because it may eventually work the lining loose.

It is assumed that the only force tending to dislodge the lining is the frictional force on the bearing surface between the lining and the shaft. This force is denoted here as F_b. The assumed criterion for no slippage is:

$$F_b < F_i \tag{3.1}$$

-where F_i is the total frictional force in the interference fit(in the case of rotary slippage, the difference in radii where these two frictional forces act may be neglected for a small w/d ratio, where w is the lining thickness and d is the bore diameter).

F_b can be approximated as follows:

$$F_b = \mu_b(\sigma_p(\pi RL)) \tag{3.2}$$

-where

σ_p = "projected-area" pressure, as estimate of bearing pressure

πRL = approximate contact area of bearing

R = radius of lining(to avoid future complications, inner radius a and outer radius b are not distinguished here, which is permissible due to the thin-wall assumption)

L = length of bearing

μ_b = coefficient of friction between lining and shaft

F_i arises from the following two causes: (1) the interference fit; (2) radial loads, from the shaft, transmitted through the lining. The former cause acts around the whole circumference, the latter only on the loaded side of the bearing. Superposing these two causes gives:

$$(3.3) \quad F_i = \mu_i(\sigma_i(2\pi RL)) + \mu_i(\sigma_p \pi RL) = \mu_i \pi RL(2\sigma_i + \sigma_p)$$

-where

μ_i = coefficient of friction in interference fit, between lining and housing

σ_i = that part of the interfacial normal pressure, in the interference fit, due to the interference only

Now σ_i will be related to the amount of interference for normal temperatures, i_n. The housing bore is here regarded as fixed in size. Also, it is assumed that, due to a thin wall, the circumferential strain may be treated as uniform through the lining. Then the desired relation, taking the interference as twice the radial displacement, is:[30]

$$(3.4) \qquad i_n = 2\frac{\sigma_i R^2}{Ew}$$

-where E = Young's modulus of lining
w = thickness of lining

or, rewriting,

$$(3.5) \qquad \sigma_i = \frac{Ew}{2R^2} i_n$$

Eq.(3.4) differs from the corresponding equation for the deformation of a cylindrical pressure vessel by the absence of a component due to axial stresses, which usually are insignificant in the interference fit here.

Substituting Eq.(3.5) into Eq.(3.3) and simplifying gives:

$$(3.6) \qquad F_i = \mu_i \pi RL\left(\frac{Ew}{R^2} i_n + \sigma_p\right)$$

Eqs.(3.6), (3.2), and (3.1) now combine to give:

$$(3.7) \qquad \mu_i \pi RL\left(\frac{Ew}{R^2} i_n + \sigma_p\right) > \mu_b \sigma_p \pi RL$$

Rearranging Eq.(3.7) and using the relation that $R = \frac{1}{2}d$, d being the diameter of the bore, gives:

$$(3.8) \qquad \frac{i_n}{d} > \left(\frac{\sigma_p}{4E}\right)\left(\frac{\mu_b}{\mu_i} - 1\right)\left(\frac{1}{w/d}\right)$$

-where, as before, w/d = relative wall thickness.

Eq.(3.8), the desired relationship, indicates the minimum amount of interference theoretically required to prevent movement of the lining. This equation is valid for both the cases of rotating and reciprocating shafts, and it is assumed that seizure of the shaft to the lining does not

occur. No interference is required by Eq.(3.8) when the coefficient of friction in the fit is higher than that on the bearing surface(however, some interference would of course be necessary in practice to hold the lining in place). Where the converse is true for the coefficients of friction, Eq.(3.8) says that the required interference is directly proportional to the bearing loads and inversely proportional to the wall thickness. There is no apparent disadvantage to having an interference higher than the minimum, so long as the lining can be pressed into the housing without too much difficulty.

The material trademarked Thordon was previously estimated to have a Young's modulus of about 50,000 psi. Assuming a typical w/d ratio of 1/10, and taking the maximum recommended load of 2,500 psi, Eq.(3.8) gives:

$$(3.9) \qquad \frac{i_n}{d} > \frac{1}{8}\left(\frac{\mu_b}{\mu_i} - 1\right)$$

It is apparent from Eq.(3.9) that the interference required for high bearing pressures would be excessive if the frictional coefficient for the bearing surface, μ_b, were even slightly greater than that for the interference fit, μ_i. The situation would be even worse for a thinner wall or a softer elastomer. Therefore, so far as anchoring the lining is concerned, it is recommended that either μ_i and μ_b be adjusted such that the former is equal to or higher than the latter(for this reason, a lubricated fit is

not recommended here), or that the lining be held by a bond or by end flanges. Bonding, unfortunately, should produce higher thermal and swelling bore contractions than a well-lubricated fit; however, dependence on high friction to hold the lining might still allow some axial lining expansion and consequently produce lower bore contractions than bonding would. One method of increasing μ_i is by introducing fine abrasive powder(like 30-micron grit size) into the fit; the compressive deflection tests showed this powder to be effective in increasing friction. In the case of end flanges, μ_i might be reduced to insure free axial expansion; this might also permit the lining to rotate in the housing, which, however, might not be objectionable here.

If the above recommendation that μ_i be made equal to or greater than μ_b is carried out, then the right side of Eq.(3.8) becomes zero or negative, making Eq.(3.8) useless for recommending an interference. Therefore, the recommendation to be given here will be in terms of the frictional holding strength of the interference fit in the absence of shaft loads, or, what basically amounts to the same thing, the force required to press-fit the lining, here called F_p, which is:

$$F_p = \mu_i(\sigma_i(2\pi RL)) \tag{3.10}$$

From Eqs.(3.5), (3.10), and noting that $R = \frac{1}{2}d$,

$$i_n = \frac{1}{2\pi\mu_i E}\left(\frac{1}{w/d}\right)(F_p/L) \tag{3.11}$$

-where F_p/L is the pressing force per unit of bearing length.

As installation difficulty increases with increasing F_p/L, F_p/L should be the minimum value that can be depended upon to hold the lining. F_p does not have to be as high as the bearing surface's forces so long as Eq.(3.8) is satisfied by having $\mu_i > \mu_b$. For example, a Thordon bearing of $1\frac{1}{2}$ in. bore, 2 in. length, $\frac{1}{4}$ in. wall thickness, and .008 in. interference(more than the amount recommended by the Thordon brochure), was found by a compression testing machine to require a total pressing force of about 600 lbs., which is considerably lower than the allowable bearing forces for this size bearing. Incidentally, this result agrees quite well with Eq.(3.11) when the estimated values $\mu_i = 0.7$, for Thordon on polished steel, and E = 50,000 psi, are used. The choice of F_p/L appears to be somewhat arbitrary, or best determined by trial and error.

For a constant bore-to-length ratio, a constant F_p/L would correspond to a linear proportionality of F_p to the bore diameter and would also mean, according to Eq.(3.11) (assuming a constant w/d), a constant i_n, regardless of bore diameter; an F_p/L proportional to the bore diameter would correspond to an F_p that varied as the square of the diameter and to an i_n that was proportional to the diameter. The latter case is approximately the one suggested by the interference chart in the Thordon brochure.

Another problem in the application of Eq.(3.11) is the difficulty in accurately specifying μ_1, which is highly dependent on such things as the elastomer's hardness, the finish of the housing bore, lubrication, additives, and the interfacial pressure.

3.2 EXTRA INTERFERENCE FOR LOW TEMPERATURES

As already mentioned, the interference fit is often the only means used to keep the lining in place. When the bearing is placed in an environment much colder than the installation temperature, thermal contraction of the outside diameter of the lining may result in loosening from the housing. The purpose of this section is to determine the additional interference necessary in the fit at installation to assure that this will not happen.

It is desired that, if the interference fit were actually measured at the lowest environmental temperature, it would still be at least the minimum considered necessary to hold the lining. Treating the lining as unhoused, the extra interference required to reach this desired condition at the lowest temperature would be equal to the thermal contraction of the lining's outside diameter. This thermal contraction can be determined by putting the temperature difference into Eq.(2.6) and multiplying by two to give the diametral change rather than the radial change. The final result is:

$$(3.12) \qquad i_L = \alpha (T_o - T_e) \cdot D$$

-where

i_L = extra interference required(to be added to the recommended interference for normal temperatures)
T_o = installation temperature
T_e = lowest environmental temperature to be encountered
D = $2b$ = outside diameter of lining
α = coefficient of thermal expansion

4. OVERALL CONCLUSIONS

4.1 DESIGN RECOMMENDATIONS

On the basis of this thesis, the following overall design recommendations are made:

(1) Minimize the lining thickness to minimize load deflections, thermal and swelling clearance requirements, and heat buildup. Very thin linings can be machined by supporting the lining in a housing while boring.

(2) Make sure that the coefficient of friction in the interference fit is at least as high as that of the bearing surfaces in order to prevent slippage of the lining at high loads. Raising the friction in the fit also reduces load deflections, particularly under high loads. The friction can be increased by spreading fine abrasive powder over the surfaces. An alternative is bonding.

4.2 SUGGESTIONS FOR FURTHER INVESTIGATIONS

One area under the subject of deflections that might be suitable for further study is the compressive behavior of very stiff elastomers, particularly at high shape factors. It is recommended that any further deflection testing for the purpose of checking theory be done with bonded slabs or at least with specimens that are bonded at all contact faces- sleeve bearings introduce into both theory and experiment too many unpredictable, hard-to-control, or complicating factors such as complex geometry, uneven pressure, and surface slippage. It should be repeated here that creep is a serious problem in the elastic testing of Thordon.

Other areas that could use some further testing are the thermal and swelling bore changes, particularly as regards the effect of bonding. Large bearings should be used for accuracy, and the measurement techniques suggested in Sec. (2.3.4) might be used.

Some areas that are outside the scope of this thesis are: (1) bearing friction and wear; (2) maximum permissible P-V(pressure times velocity) values; (3) the distribution of bearing pressure over the contact area. However, the first two of these areas in particular would probably not be found to be suitable for an extensive purely theoretical treatment, and the number of variables they would involve might make testing a great undertaking.

BIBLIOGRAPHY

1. McPherson, A.T., and Klemin, Alexander(editors). Engineering Uses of Rubber. New York: Reinhold Publishing Corp., 1956. Page 83

2. Ibid.

3. Harris, Cyril M., and Crede, Charles E.(editors). Shock and Vibration Handbook. New York: McGraw-Hill, 1961. Volume 2, page 35-21

4. Gorelik, B.M., Bukhina, M.F., and Ratner, A.V., "Study of the Compression of Circular Rubber Rings and Cylinders," Soviet Rubber Technology II, No. 22 (1960, translation of the Russian journal Kauchuk i Rezina).

5. Davey, A.B., and Payne, A.R. Rubber in Engineering Practice. London: Maclaren & Sons; New York: Palmerton Publishing Co. 1964. Page 6

6. Ibid., pp. 89-90

7. Allen, P.W., Lindley, P.B., and Payne, A.R.(editors). Use of Rubber in Engineering. London: Maclaren & Sons, 1967. Page 6

8. Payne, A.R., and Scott, J.R. Engineering Design with Rubber. London: Maclaren & Sons; New York: Interscience Publishers, 1960. Page 8

9. Fung, Y.C. A First Course in Continuum Mechanics. Englewood Cliffs, New Jersey: Prentice-Hall, 1969. pp. 163-165

10. Davey & Payne, op. cit., page 116.

11. Harris & Crede, op. cit., page 35-15.

12. Gent, A.N., and Lindley, P.B., "The Compression of Bonded Rubber Blocks," Proc. Inst. Mech. Engrs. CLXXIII, No. 3 (1959), pp. 111-117

13. McPherson & Klemin, op. cit., page 80.

14. Gent & Lindley, op. cit.

15. Ibid.

16. Fung, op. cit.

17. Harris & Crede, op. cit.

18. Gorelik, Bukhina, & Ratner, op. cit.

19. Gent & Lindley, op. cit.

20. Ibid.

21. Recommended by: Badische Analin-Soda Fabrik (BASF) Ludwigshafen-Rhine, Federal Republic of Germany

22. Payne & Scott, op. cit. page 65

23. Boley, Bruno A., and Weiner, Jerome H. Theory of Thermal Stresses. New York: John Wiley & Sons, 1960. Page 291

24. Timoshenko and Goodier, Theory of Elasticity. New York: McGraw-Hill, 1951. Art. 134, page 407

25. Ibid., art. 135, page 408

26. Ibid., art. 135, page 414

27. Ibid., art. 135, page 409

28. Boley & Weiner, op. cit.

29. Timoshenko & Goodier, op. cit., art. 135, page 412

30. Nash, William A. Theory and Problems of Strength of Materials. New York: Schaum Publishing Co., 1957. pp. 38-40